CENTER FOR DRUG EVALUATION AND RESEARCH

APPLICATION NUMBER:

22-059

PHARMACOLOGY REVIEW(S)

MEMORANDUM
March 12, 2007

TO: File
FROM: Kenneth L. Hastings, Dr.P.H., D.A.B.T.

SUBJECT: NDA 22-059

I concur with Dr. Kimberly Benson and Dr. John Leighton that the marketing application for lapatinib (Tykerb®) may be approved based on review of submitted nonclinical data. Pregnancy Category D is appropriate based on the high rate of pup lethality observed in reproductive toxicology studies with rats. I also concur that the Sponsor should conduct Phase 4 studies to determine the cause of this high rate of newborn mortality.

_____
Kenneth L. Hastings, Dr.P.H., D.A.B.T.
Associate Director
Office of New Drugs

This is a representation of an electronic record that was signed electronically and this page is the manifestation of the electronic signature.

/s/

Kenneth Hastings
3/12/2007 05:25:31 PM
PHARMACOLOGIST

MEMORANDUM

Date: March 5, 2007
From: John K. Leighton, Ph.D., DABT
Supervisory Pharmacologist
Division of Drug Oncology Products
To: File for NDA #22-059
TYKERB (lapatinib)
Re: Approvability for Pharmacology and Toxicology

Nonclinical studies that investigated the pharmacology and toxicology of lapatinib provided to support the NDA for TYKERB for the treatment of advanced or metastatic breast cancer, in combination with capecitabine, in patients whose tumors overexpress HER2, were reviewed in detail by Dr. Kimberly Benson. The supporting information included studies of lapatinib that investigated the drug's pharmacology, alone and in combination with capecitabine; pharmacokinetic and ADME; safety pharmacology; general toxicology (mouse, rat and dog); genetic toxicity (complete ICH battery); genetic toxicity of an impurity —— ;eproductive toxicity in both rats and rabbits; and special toxicology studies of local tolerance. The studies cited in the review by Dr. Benson consist of original research conducted by the applicant.

The general toxicology studies submitted to the NDA demonstrate that lapatinib is well tolerated in rats and dogs, and no unusual findings were noted. In genetic toxicity studies, an impurity with a structural alert was found to be genotoxic in *in vitro* assays. The sponsor is investigating the carcinogenic potential of lapatinib; it is not clear if the batches of lapatinib to be used in those studies include appropriate levels of the impurity. However, these studies will not impact the approvability of TYKERB for the proposed indication.

Lapatinib was negative for significant effects on fertility and embryo-fetal development. However, in the rat pre and postnatal toxicity study, Dr. Benson reported the toxicity to pups shortly after birth that had been exposed *in utero* to lapatinib. This unusual finding is of concern and remains unexplained. Dr. Benson requested additional follow-up, but this is not required for approval or as a phase 4 commitment. Both issues were adequately addressed by Dr. Benson. Finally, an effect on QT prolongation was noted in a clinical study with TYKERB. If additional evaluations on cardiovascular function are warranted, a HERG assay, which was not performed to date in development, may provide useful information. This was also noted in Dr. Benson's review.

Recommendations: I concur with Dr. Benson's conclusion that pharmacology and toxicology data support the approval of NDA 22-059, TYKERB. There are no outstanding nonclinical issues related to the approval of TYKERB.

This is a representation of an electronic record that was signed electronically and this page is the manifestation of the electronic signature.

/s/

John Leighton
3/5/2007 06:04:39 PM
PHARMACOLOGIST

DEPARTMENT OF HEALTH AND HUMAN SERVICES
PUBLIC HEALTH SERVICE
FOOD AND DRUG ADMINISTRATION
CENTER FOR DRUG EVALUATION AND RESEARCH

PHARMACOLOGY/TOXICOLOGY REVIEW AND EVALUATION

NDA NUMBER:	**22-059**
SERIAL NUMBER:	**000**
DATE RECEIVED BY CENTER:	**8/25/06**
PRODUCT:	**Tykerb ® (lapatinib)**
INTENDED CLINICAL POPULATION:	**Metastatic breast cancer, in combination with capecitabine**
SPONSOR:	**GlaxoSmithKline**
DOCUMENTS REVIEWED:	**Electronic Submission**
REVIEW DIVISION:	**Division of Drug Oncology Products**
PHARM/TOX REVIEWER:	**Kimberly A. Benson, Ph.D.**
PHARM/TOX SUPERVISOR:	**John K. Leighton, Ph.D.**
DIVISION DIRECTOR:	**Robert Justice, MD**
PROJECT MANAGER:	**Kim Robertson**

Date of review submission to Division File System (DFS): 5 March 2007

TABLE OF CONTENTS

EXECUTIVE SUMMARY

I. Recommendations

A. Recommendation on approvability
Approvable. The non-clinical studies with oral lapatinib support the safety of its use in metastatic breast cancer.

B. Recommendation for nonclinical studies
No additional non-clinical studies are required for lapatinib. However the Sponsor should consider further reproductive toxicology studies to attempt to determine the nature of the toxicity that was seen in the pre- and post-natal development study in the rat. A 91% lethality rate in the offspring of rats given a dose of 120 mg/kg was seen by Post Natal Day (PND) 4. A similar level of lethality was seen when another study when *in utero*-exposed offspring, fostered on PND 0 to non-treated dams still showed significant lethality within the first week of life. Further investigation into a possible cause of death in the pups and into whether there is a critical time in gestation for lapatinib dosing to yield this toxicity.

Should QT prolongation adverse events become more prevalent when Tykerb use increases once the drug is approved, the sponsor may consider conducting a hERG assay. This could identify and IC_{50} for the inhibition of the hERG channel.

C. Recommendations on labeling
The recommendations to the sponsor's proposed labeling are given, with a detailed report regarding the rationale for the recommended changes, in a subsequent review.

II. Summary of nonclinical findings

The nonclinical findings have shown the target sites of toxicity with lapatinib to be gastrointestinal, hepatobiliary, adrenal and dermatological. Many of these toxicities are seen in the clinic and are direct effects of the pharmacology of lapatinib.

Lapatinib was not mutagenic or clastogenic in the *in vitro* and *in vivo* assays studied. An impurity present in the formulation of lapatinib at levels exceeding recommended levels for genotoxic impurities tested positive for genotoxicity in two *in vivo* assays.

Lapatinib did not impair fertility when administered to either male or female rats prior to and during the mating time frame. It was not teratogenic in either the rat or the rabbit. It did, however, lead to a dramatic increase in neonatal loss in rats during the first week of life.

A. Pharmacologic activity

The pharmacological activity of lapatinib is inhibition of EGFR and erbB-2 tyrosine kinase phosphorylation. Studies in cell lines and enzyme assays have both shown that lapatinib inhibits EGFR and erbB-2 at concentrations significantly lower than those needed to inhibit *c-src*, VEGFR-2, CDK-2, CDK-4 and erbB-4.

Lapatinib showed activity in several mouse xenograft models. Inhibition of tumor growth, and in some cases decreased tumor size, was seen with lapatinib administration to the mice injected with tumor cell lines.

An *in vitro* study investigating the cell growth inhibition of lapatinib combined with 5-FU, the active metabolite of capecitabine, was conducted. This study was conducted in four human tumor cell lines that were chosen specifically because they express low levels of erbB-2 (a target of lapatinib) and also yield a weak growth inhibition response to lapatinib alone. The information from the dose-response curves were then used in an analysis that was a modified version of the Chou and Talalay combination index analysis to determine a combination index (CI), which is a measure of additive, synergy or antagonism. A number, though not all, of the dose-response curves obtained show an improved response to the combination of lapatinib + 5FU compared to either agent alone. The CI values obtained ranged from 0.84 to 1.14, with a CI of ~1 suggestive of an additive effect.

B. Nonclinical safety issues relevant to clinical use

Nonclinical pharmacokinetic studies with lapatinib have shown that the oral bioavailability ranges from 42-50%. Metabolism primarily involves the P450 isozymes CYP3A4 and CYP3A5. Induction of these enzymes does not appear to be occurring with lapatinib exposure. The primary excretion route of lapatinib is fecal, as mass balance studies show minimal recovery in the urine and the majority of the drug and metabolite recovery in the feces. Tissue distribution studies have shown lapatinib is not greatly absorbed orally and primarily found in the GI tract and at 4 hrs after administration to rats. The tissues with small but significant amounts of lapatinib had relatively equivalent distribution of the drug, with little transport across the blood-brain-barrier. Protein binding of lapatinib was very similar across species, with mice, rats, dogs and humans showing > 99 % of lapatinib bound to plasma proteins. The metabolic profiles of lapatinib are very similar in the rat, dog and human.

The final Tykerb drug product contains several impurities that exceed acceptable limits, including two with structural alerts, [redacted], as well as [redacted] Certificate of Analyses were not provided for all the toxicology reports, only the two long-term (rat and dog) studies. The impurities of concern were present in the formulations used in these studies, though not at levels that would qualify the substances. However, the animal studies utilized doses high enough that the animals were exposed to levels exceeding the clinic levels, on a body surface area basis. In addition, the Sponsor has ongoing carcinogenicity studies in the rat and mouse where, provided adequate levels

of these components of the final drug product are present, will address the issue with life-time exposure in the laboratory.

The nonclinical safety issues seen in the toxicology program with lapatinib were mostly toxicities that could be suspected from a drug of this class. Skin lesions and reddening, seen in the rat and dog, are known actions of drugs of this class. Other EGFR tyrosine kinase inhibitors have this same effect and skin rashes are a primary toxicity seen in man

Clinically, the DLT for lapatinib has been gastrointestinal. Diarrhea, including severe diarrhea, is the primary toxicity with Tykerb administration, though treatment can usually continue with concomitant anti-diarrheal medication. The GI is a primary site of toxicity in the non-clinical animal models as well. Although emesis and diarrhea were not widely seen in the toxicology studies, and loose stools were only noted in the rabbit, there were still significant histopathological changes on the GI, including degeneration and inflammation. This is likely an extension of the pharmacological action of lapatinib at the EGFR receptors of the gastrointestinal mucosa.

Of recent concern with drugs that inhibit the tyrosine kinases is cardiovascular toxicity, and a clinical report with Tykerb showed QT prolongation. No indications of this toxicity were seen in the animal models. Heart weights were not increased, absolute or weights relative to animal body weight, except in a LD group in the long-term dog study. Histopathological changes in the hearts of rats and dogs were noted, but they were of a very low frequency. These included focal fibrosis, infiltration and myocyte degeneration of the heart in rats and one dog with hemorrhage noted in the heart. The rat finding was not replicated in a longer-term study at the same dose. In general, these results are not indicators of a strong possibility of potential cardiac toxicities from Tykerb in the clinic, though vigilance in monitoring the potential is warranted until more clinical experience is gained. If with increased clinical experience with Tykerb increased QT prolongation events are seen, a hERG assay may be helpful to identify the IC_{50} for the channel inhibition.

Also of interest with drugs that act to inhibit tyrosine kinases has been ocular toxicity. In the studies with lapatinib, there was little evidence of this. The only noted eye toxicities were muscular, with damage to the eye skeletal muscle seen; no corneal or retinal damage was found.

The hepatobiliary system is another site of toxicity of lapatinib in the animal models. Rat studies showed liver inflammation and hepatocellular hypertrophy and slight increases in transaminase and bile acids. This was seen in studies of shorter duration but not in the pivotal long-term rat study. In the dog there was chronic liver inflammation, increased liver weights, hepatocellular necrosis/degeneration, cholestasis, elevated bilirubin, bile acids and transaminases. However this toxicity has not been seen in clinical trials.

The reproductive toxicity of most concern was a striking decrease in neonatal viability. While there was no difference in the number of viable fetuses born, lapatinib led to 91% of the offspring dying within the first four days of life at an AUC approximately 6 times

that seen clinically in a lapatinib + capecitabine study. Given the histological changes seen in the mammary glands in other toxicology studies and the involvement of erbB-2 in mammary gland development and because the pups that died did not have milk in their stomachs a cross-fostering study was done to factor out of the equation the treated-mother during lactation. Again up to 84% of pups exposed *in utero* to lapatinib still died, despite being nursed by dams that had never been exposed to lapatinib. This information is important for physicians when counseling their patients regarding pregnancy and Tykerb administration.

The toxicities of lapatinib in nonclinical models are generally not severe and are expected as direct pharmacological actions of an EGFR tyrosine kinase inhibitor.

The majority of the toxicities seen with lapatinib are most likely an extension of the pharmacological action of the drug.

2.6 PHARMACOLOGY/TOXICOLOGY REVIEW

2.6.1 INTRODUCTION AND DRUG HISTORY

NDA number:	**22-059**
Review number:	1
Sequence number/date/type of submission:	01/13 September 2006/Electronic NDA
Information to sponsor:	Yes ( ) No (X)
Sponsor and/or agent:	GlaxoWellcome Five Moore Drive PO Box 13398 Research Triangle Park, NC 27709-3398
Manufacturer for drug substance:	Glaxo Operations UK Limited Priory Street Ware Herfordshire SG12 0DJ United Kingdom

Reviewer name:	Kimberly A. Benson, Ph.D.
Division name:	Division of Drug Oncology Products
Review completion date:	5 March 2007

Drug:

Trade name:	Tykerb®
Generic name:	Lapatinib ditosylate
Code name:	GW572016 GW572016X – free base GW572016F – ditosylate salt GW572016B –
Chemical name:	*n*-{3-chloro-4-[(3-fluorobenzyl)oxy]phenyl}-6-[5-({[2-(methylsulfonyl)ethyl]amino}methyl)-2-furyl]quinazolin-4-amine bis(4-methylbenzenesulfonate) monohydrate
CAS registry number:	388082-78-8
Molecular formula/molecular weight:	$C_{29}H_{26}ClFN_4O_4S(C_7H_8O_3S)_2H_2O$/943.48

Structure:

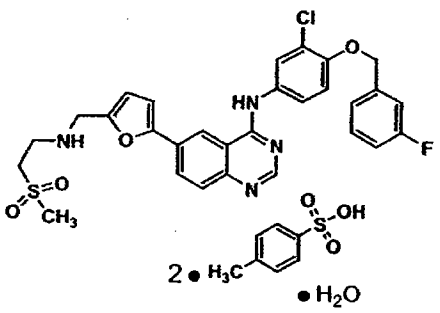

Relevant INDs/NDAs/DMFs: IND 61,362

Drug class: Tyrosine kinase inhibitor

Intended clinical population: TYKERB is indicated in combination with capecitabine for the treatment of patients with advanced or metastatic breast cancer whose tumors overexpress HER2) and who have received prior therapy including an anthracycline, a taxane, and trastuzumab.

Clinical formulation:

Table 1 Composition of Lapatinib Tablets, 250 mg

Component	Quantity (mg/tablet)	Function	Reference to Standard
Lapatinib Ditosylate [1] Microcrystalline Cellulose [2] Povidone	405.0	Active	GSK Specification NF USP
Weight			
Core Tablet			
Sodium Starch Glycolate Magnesium Stearate Core Tablet Weight			NF NF
Film Coating			
Orange		Film Coat	Supplier
Total Coated Tablet Weight		-	-

Notes:

[Table excerpted from Sponsor]

Route of administration: Oral

Disclaimer: Tabular and graphical information are constructed by the reviewer unless cited otherwise.

Data reliance : Except as specifically identified below, all data and information discussed below and necessary for approval of 22-059 are owned by GlaxoSmithKline or are data for which GlaxoSmithKline has obtained a written right of reference. Any information or data necessary for approval of 22-059 that GlaxoSmithKline does not own or have a written right to reference constitutes one of the following: (1) published literature, or (2) a prior FDA finding of safety or effectiveness for a listed drug, as described in the drug's approved labeling. Any data or information described or referenced below from a previously approved application that GlaxoSmithKline does not own (or from FDA reviews or summaries of a previously approved application) is for descriptive purposes only and is not relied upon for approval of 22-059.

Studies reviewed within this submission:

PHARMACOLOGY

Primary Pharmacodynamics

RR2000/00018/00: Inhibition of epidermal growth factor receptor and ErbB-2 tyrosine kinase activity by GW572016B

RD2006/00999/00: A unique structure for epidermal growth factor bound to GW572016 (lapatinib): Relationships among protein conformation, inhibitor off-rate, and receptor activity in tumor cells

RR2000/00019/01: GW572016B is a highly selective inhibitor of epidermal growth factor receptor and ErbB-2 tyrosine kinase activities

RH2001/00009/01: The effects of GW572016 on the phosphorylation state of epidermal growth factor receptor, ErB-2, AKT and p42/44 ERK in the HN5 and BT474 cell lines

RH2006/00069/01: Regulation of survivin protein by GW572016

RR2000/00003/01: The effects of GW572016 on the growth of human normal and transformed cell lines

RH2003/00020/00: The effects of compound dilution protocol and salt form on the reported cellular growth inhibition properties of GW572016

RC2006/00095/00: Assessment of tumor cell growth inhibition by the combination of lapatinib ditosylate (GW572016F) and 5-fluorouracil (5-FU)

RR2000/00021/02: Antitumor activity of GW572016B in the ErbB-2 positive BT474 human breast cancer xenograft

Secondary Pharmacodynamics

RR2000/00069/00: Secondary pharmacological evaluation of the dual ErbB-2 tyrosine kinase inhibitor GW572016B in radioligand binding and isolated tissues assays.

Safety Pharmacology

RD2000/00236/00: GW572016F: Safety pharmacology study of overt central and peripheral pharmacodynamic effects following single-dose oral administration in conscious female Wistar Han rats.
RD2000/00237/00: GW572016F: Safety pharmacology study of overt central and peripheral pharmacodynamic effects following single-dose oral administration in conscious beagle dog.
WD2000/00426/00: GW572016B (ErbB-2 inhibitor) Safety pharmacology: cardiovascular effects following acute intraduodenal administration in anaesthetized Wistar Han rats.
RD2000/00143/01: GW572016F: Evaluation of cardiovascular (hemodynamic) functions following acute oral administration to conscious telemetered male Wistar Han rats.
RD2000/00144/00: GW572016F: Airway resistance and dynamic lung compliance in male guinea pigs.
RD2000/01107/00: GW572016F: Evaluation of cardiovascular (hemodynamic) functions following acute oral capsule administration to conscious telemetered male beagle dogs.
RR2000/00076/00: The effects of GW572016F on canine Purkinje fiber action potentials.

PHARMACOKINETICS/TOXICOKINETICS

Analytical Methods and Validation Reports

None reviewed

Absorption

RD2000/00063/00: Single dose pharmacokinetics of GW572016F in male CD mice, Han Wistar rats and beagle dogs after intravenous and oral administration
RD2000/00696/00: Single and repeat dose pharmacokinetics of GW572016F in female CD-1 nude mice after oral administration for up to 14 days
RD2000/00327/00: Pharmacokinetics of GW572016X following intravenous and oral administration of GW572016F to male rats
RD2000/02336/00: Pharmacokinetics of GW572016X following oral administration of GW572016F and GW572016X to male Wistar Han rats
RD2000/00321/00: Pharmacokinetics of GW572016X following intravenous and oral administration of GW572016F to male beagle dogs
RD2000/02334/00: Pharmacokinetics of GW572016X following oral administration of GW572016Fand GW572016X at 10 mg/kg GW572016X to male beagle dogs

Distribution

RD2000/00355/01: The *in vitro* binding of GW572016X to plasma proteins and erythrocyte partitioning in mouse, rat, rabbit, dog and human
RD1999/02816/00: ^{14}C-GW572016: Quantitative wholebody autoradiography following oral administration (10 mg[base]/kg) to the albino and pigmented rat

Metabolism

In Vitro Metabolism

RD2000/01947/00: *In vitro* metabolism of GW572016 using 1) heterologously-expressed recombinant human CYP450 enzymes and 2) pooled human liver microsomes with a CYP3A4/5 selective inhibitor

RD2005/00052/00: An *in vitro* investigation of the enzymes involved in the formation of alkylamine N-oxidation metabolites of 14C-GW572016 using human liver microsomes and heterologously expressed human cytochrome P450 and flavin-containing monooxygenase enzymes

RD2002/01185/00: An *in vitro* evaluation of the inhibitory potential of GW572016 on human cytochrome P450 enzymes

RD2001/01300/00: An *in vitro* evaluation of the inhibitory potential of GW572016 on testosterone 6b-hydroxylase and midazolam 1-hydroxylase activity in human liver microsomes

RD2004/00416/00: An *in vitro* evaluation of GW572016 as an inducer of cytochrome P450 expression in cultured human hepatocytes

In Vivo Metabolism

RD2004/02884/00: Quantitative Metabolite Profiling and Metabolite Identification in Plasma, Bile and Feces of CD-1 Mice Administered [14C]-GW572016 Orally as a Suspension at 30 mg free base/kg

RD2003/00475/01: Profiling and identification for metabolites of GW572016 in the Sprague-Dawley rat following a single oral administration of 14C-GW572016 at 10 mg free base/kg

RD2004/01115/00: Metabolite Profiling Identification in Plasma and Feces of Rats Administered [14C]-GW572016 Orally as a Suspension at 10 mg free base/kg

RD2002/00072/00: Identification of the metabolites of GW572016 in the dog

RD2004/00932/00: Profiling and identification for metabolites of GW572016 in humans after single oral administration of 14C-GW572016

RD2003/00727/02: GW572016: Radioanalysis of samples following single 250 mg oral suspension dose of [14C]-GW572016 to healthy volunteers 7274-208

Excretion

RD2004/01116/00: Elimination of radioactivity following a single oral administration of ^{14}C-GW572016 to male and female intact and male bile duct cannulated mice

RD2002/01538/00: Elimination of radioactivity following a single oral (10 mg/kg) administration of ^{14}C-GW572016 to male and female intact and male bile duct-cannulated rats

RD2000/00324/00: Absorption, distribution, metabolism, and elimination of ^{14}C-GW572016X following intravenous and oral administration to male beagle dogs

Pharmacokinetic Drug Interactions (Non-clinical)
RD2002/00921/00: The *in vitro* inhibition of GW572016X metabolism by paclitaxel, docetaxel and vinorelbine in pooled human liver microsomes
RD2001/01665/00: The inhibition of paclitaxel, docetaxel, and vinorelbine metabolism by GW572016X in pooled human liver microsomes
RD2002/01031/00: An *in vitro* study to examine GW572016 and Iressa interactions with paclitaxel metabolism

TOXICOLOGY

Single-dose Toxicity
Mouse
RD2000/00398/00: GW572016F: Single-dose intravenous toxicity study in CD-1® mice
RD2000/00192/00: GW572016F: Single-dose oral toxicity study in CD-1® mice
Rat
RD2000/00479/00: GW572016F: Single-dose intravenous toxicity study in Wistar Han rats
RD1999/02824/00: GW572016F: Single-dose oral toxicity study in Wistar Han rats

Repeat-dose Toxicity
Mouse
RD2001/01439/00: GW572016F: 14-Day oral gavage dose-range-finding toxicity study in CD-1 mice.
RD2002/01283/00: GW572016F: 13-Week oral gavage pilot carcinogenicity study in mice.

Rat
RD1999/01207/00: GW572016B and GW574783B: Non-audited 7-day toxicity study in male Han Wistar rats.
RD1999/02391/00: GW572016F: 14-Day oral gavage toxicity study in Wistar Han rats.
RD2000/01171/01: GW572016F: 13-Week oral toxicity study in Wistar Han rats.
RD2001/01306/00: GW572016F: A 26-Week oral gavage toxicity study in Wistar Han rats.

Dog
RD1999/01838/01: GW572016B:Non-audited 7-day oral toxicity study in male Beagle dogs.
RD1999/02634/00: GW572016 F: 14-Day oral toxicity study in Beagle dogs.
RD2000/01600/01: GW572016F: 13-Week oral toxicity study in Beagle dogs.
RD2001/00926/01: GW572016F: 39-Week oral capsule toxicity study in beagle dogs.

Genotoxicity
In Vitro
RD1999/01825/00: Bacterial mutagenicity report

RD2000/00409/01: GW572016F: *Salmonella* and *E. coli*/ Microsome standard plate incorporation assay (study V40754)
RD2000/00306/00: Mouse lymphoma mutagenicity report (non-GLP)
RD2000/00577/00: GW572016F: *In vitro* assay for chromosomal aberrations in Chinese Hamster Ovary (CHO) cells (study V40736)
RD2000/01529/00: GW572016F: *In vitro* assay for chromosomal aberrations in cultured human peripheral blood lymphocytes (Study V40806)

In Vivo
RD2000/01601/00: GW572016F: Chromosomal aberrations *in vivo* in rat bone marrow cells (Study R40807)

Reproductive and Developmental Toxicity
Fertility and Early Embryonic Development
CD/2002/00007/00: GW572016F: Oral male fertility study in rats
CD/2002/00032/00: GW572016F: Oral study of female fertility and early embryonic development to implantation in rats

Embryo-Fetal Development
WD/2001/00235/00: GW572016F (ErbB2 inhibitor): Study to determine the maximum repeatable daily oral dose in pregnant Wistar Han rats.
WD/2001/00236/00: GW572016F (ErbB2 inhibitor): A further study to determine the maximum repeatable daily oral dose in pregnant Wistar Han rats.
WD/2001/00237/00: GW572016F (ErbB2 inhibitor): Oral embryofetal development study in the pregnant Wistar Han rat.
RD/2000/00574/00: GW572016F: Non-audited dose-range finding toxicity study in non-pregnant New Zealand white rabbits.
WD/2000/00414/00: GW572016F (ErbB2 inhibitor): Study to determine the maximum repeatable daily oral dose in the New Zealand white rabbit.
WD/2000/00520/00: GW572016F (ErbB2 inhibitor): Maximum repeatable dose study in the pregnant New Zealand white rabbit.
RD/2001/00010/00: GW572016F: Oral (gavage) embryo-fetal development study in New Zealand white rabbits.

Prenatal and Postnatal Development
CD/2003/00331/00:GW572016F: Oral pre- and postnatal development study in rats.
CD/2004/00609/00:GW572016F: Oral cross-fostering study in rats.

Local Tolerance
RD2000/00530/00: GW572016F: Acute dermal irritation study in the New Zealand White rabbit
RD2000/00531/00: GW572016F: Acute eye irritation study in the New Zealand White rabbit
RD2000/00532/00: GW572016F: Skin sensitization (Magnusson-Kligman) study in the guinea pig

Other Toxicity Studies

Immunotoxicity

CD2004/00055/00: GW572016F: Effect on anti-KLH antibody response in a 28-day oral dose immunotoxicity study in the rat

Mechanistic Studies

NONE

Impurities (studies reviewed in relevant sections)

RD2006/01224/00 Acute oral toxicity in the rat – fixed dose method
RD2005/00355/00: Twenty-eight day repeated dose oral (gavage) toxicity study in the rat
RD2005/01535/00: Acute oral toxicity in the rat – fixed dose method
RD2005/00328/00: Reverse mutation assay "Ames test" using *Salmonella typhimurium*
RD2005/00329/00: Screening L5178Y TK+/- mutation assay
RD2003/01997/00: Micronucleus test in the mouse
WD2005/00458/00: Oral rat bone marrow micronucleus assay
WD2005/00898/00: Unscheduled DNA synthesis assay in rat hepatocytes following oral dosing
RD2003/00061/00: Rabbit enucleated eye test
RD2005/01536/00: Acute dermal irritation in the rabbit
RD2003/00063/00: Rabbit enucleated eye test
RD2005/01537/00: Acute eye irritation in the rabbit
RD2005/01538/00: Skin sensitization in the guinea pig – Magnusson and Kligman maximization method

Studies not reviewed within this submission:

4 Page(s) Withheld

1 Trade Secret / Confidential

_____ Draft Labeling

_____ Deliberative Process

2.6.2 PHARMACOLOGY

2.6.2.1 Brief summary

Many tumors express epidermal growth factor receptor (EGFR) and ErbB-2, closely related members of the tyrosine kinase receptor type1 family. Over-expression of EGFR and ErbB-2 is associated with poor prognosis and reduced overall survival. A drug that inhibits both EGFR and ErbB-2 could potentially be advantageous to patients whose tumors over-express either receptor and especially to those whose tumors over-express both. GW572016 (lapatinib) was developed for use in oncology due to its dual inhibition of EGFR and ErbB-2. *In vitro* and *in vivo* studies were conducted with lapatinib (GW572016: ' = GW572016B and the ditosylate monohydrate salt= GW572016F) to assess the mechanism of action, as well as the drug effects on tumor cell growth inhibition and tyrosine phosphorylation. Studies including investigating the effects of lapatinb on several human tumor cell lines were used both in cell culture and transfected into SCID mice, including the ductal breast cancer line BT454.

As proof of the mechanism of action, lapatinib was tested for its ability to inhibit purified EGFR or erbB-2 enzyme's ability to catalyze the transfer of a phosphate group from ATP to a tyrosine residue on a synthetic peptide substrate. This phosphorylation is inhibited by lapatinib with both enzymes, with IC_{50} values of 10.8 nM for EGFR and 9.2 nM for erbB-2.

Lapatinib was also tested in a screen of sixteen other protein kinases including VEGFR-2, cSrc, Raf/MEK/ERK, CDK-4/Cyclin A and erbB-4. Enzymes that lapatinib inhibited at 50% or more relative to control were further tested and IC_{50} values obtained. Results indicated IC_{50} values greater than 10 μM for the majority. Lapatinib inhibited erbB-4 with an IC_{50} = 0.36 μM and inhibited cSrc, a non-receptor tyrosine kinase, with an IC_{50}=3.5 μM, both below the values previously seen for EGFR and erbB-2.

Tumor cell lines were used to examine the effects of lapatinib on cell growth inhibition *in vitro* and *in vivo*. These cell lines included HN5 (human squamous cell head and neck cancer), BT474 (human breast carcinoma), N87 (human gastric carcinoma), and HB4a c5.2 (erbB-2 transfected breast epithelial cells). Growth inhibition *in vitro*, as measured by a methylene blue assay, showed lapatinib IC_{50} values around 0.03 μM in the transformed cell lines and 6-7 μM in normal cell lines. A screen of 49 human normal and transformed cell lines and lapatinib's ability to inhibit cell growth yielded lapatinib IC_{50} ranges of 0.025 – 11.5 μM, with the lower IC_{50} values seen in breast, gastric, lung and head/neck tumor tissues. HN5 (IC_{50}=0.029 μM) and BT474 (μM) were the most sensitive to lapatinib-induced growth inhibition.

As lapatinib is being proposed for indication with capecitabine, an additional *in vitro* study investigating the cell growth inhibition of lapatinib combined with 5-FU, the active metabolite of capecitabine, was conducted. This study was conducted in four human tumor cell lines that were chosen specifically because they express low levels of erbB-2

(a target of lapatinib) and also yield a weak growth inhibition response to lapatinib alone. The cell lines were incubated with lapatinib and 5-FU alone or in combination and dose-response curves for cellular proliferation were obtained. The low sensitivity to lapatinib alone is evident in several of the experiments. The information from the dose-response curves were then used in an analysis that was a modified version of the Chou and Talalay combination index analysis to determine a combination index (CI), which is a measure of additive, synergy or antagonism. A modified version of this analysis was conducted due to irregular shapes of some of the dose-response curves obtained in this study. A number, though not all, of the dose-response curves obtained show an improved response to the combination of lapatinib + 5FU compared to either agent alone. The CI values obtained ranged from 0.84 to 1.14, with a CI of ~1 indicative of an additive effect. The results of this study show that there may be some benefit of the combination of the two drugs in these cell lines.

When SCID mice were transfected with the transformed cell lines, lapatinib led to *in vivo* cell growth inhibition as measured by decreases in tumor weight as well as a decrease in the measurement of erbB-2 tyrosine phosphorylation.

Secondary pharmacodynamic evaluation with lapatinib tested the radioligand binding of the compound. A screen of 38 binding sites (pharmacological receptors and ion channels) indicated that lapatinib, at a concentration of 30 μM, significantly displaced ≥ 50%) specific radioligands from only five of the intended binding sites. Further studies to characterize the binding at these sites were done with a range of lapatinib concentrations and an isolated tissue assay. IC_{50} values at these sites (sigma receptor, dopamine and noradrenergic transporters, sodium and calcium channels) for GW572016 ranged from 1-26 μM, below the previous determination of an IC_{50} around 10 nM for EGFR/erb-2.

Safety pharmacology studies were conducted to investigate the effects of lapatinib on cardiovascular, overt central and peripheral neurological and pulmonary functioning. No effects were seen in the studies on the pulmonary function (guinea pig) and overt peripheral and central effects (rat), under the conditions of the studies. Cardiovascular effects of lapatinib were studied in the rat, conscious dog and canine Purkinje fibers. Increased blood pressures were seen in the dog, though still within historical ranges. This could be due to lower than average pressures seen in the vehicle group, but a drug effect should not be ruled out. In both the rat and dog studies, there were single animal anomalies seen in the results, with one MD rat showing premature ventricular contractions and one LD dog showing 3 ventricular extrasystoles approximately 1 hr after the time that Tmax would likely have been reached. Due to the single animals, neither at the highest dose tested, it is unlikely to be a lapatinib effect, though it can't be completely ruled out. Given the concern with tyrosine kinase inhibitors and the fact that QT prolongation has been seen in a clinical study with Tykerb, a hERG assay may have added some information regarding this toxicity.

2.6.2.2 Primary pharmacodynamics

Mechanism of action:
RR2000/00018/00: Inhibition of epidermal growth factor receptor and ErbB-2 tyrosine kinase activity by GW572016B

The baculovirus expression system was used to examine the effects of GW572016 on epidermal growth factor receptor (EGFR) and ErbB-2. The baculovirus expression system was used to produce the intracellular domains of human EGFR and ErbB-2 and then GW572016 was examined for its ability to impact the phosphorylation of an exogenous peptide substrate by EGFR and ErbB-2.

The figure below shows the inhibition of ErbB-2 catalyzed peptide phosphorylation by GW572016 followed by a second figure showing the inhibition of EGFR catalyzed peptide phosphorylation. The IC_{50} value, averaged from two experiments, was 9.2 ± 0.75 nM for inhibition of EGFR and the two experiment average for the IC_{50} for inhibition of ErbB-2 was 10.8 ± 0.53 nM. These figures are data from one of each of the experiments.

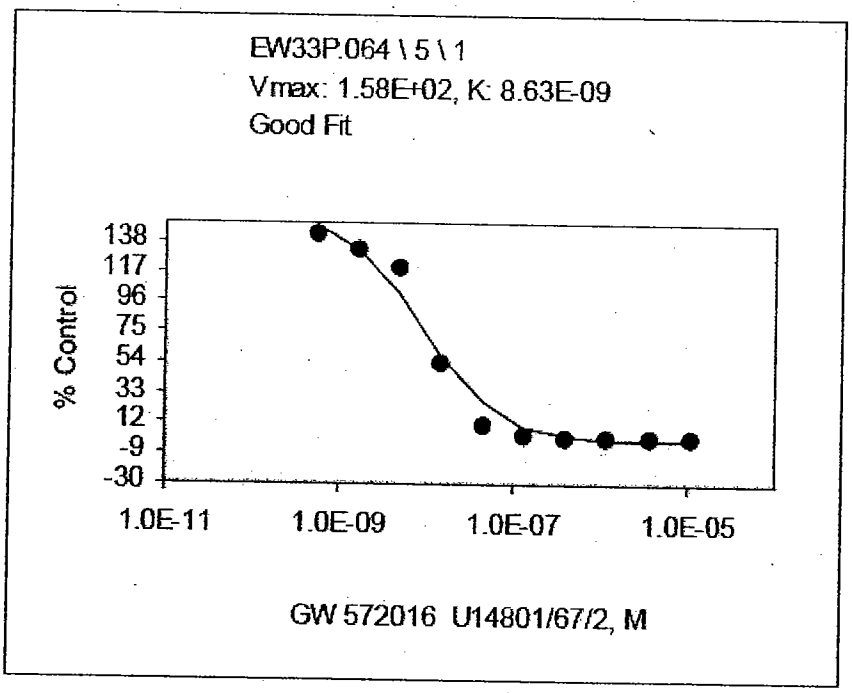

[Figure excerpted from sponsor]

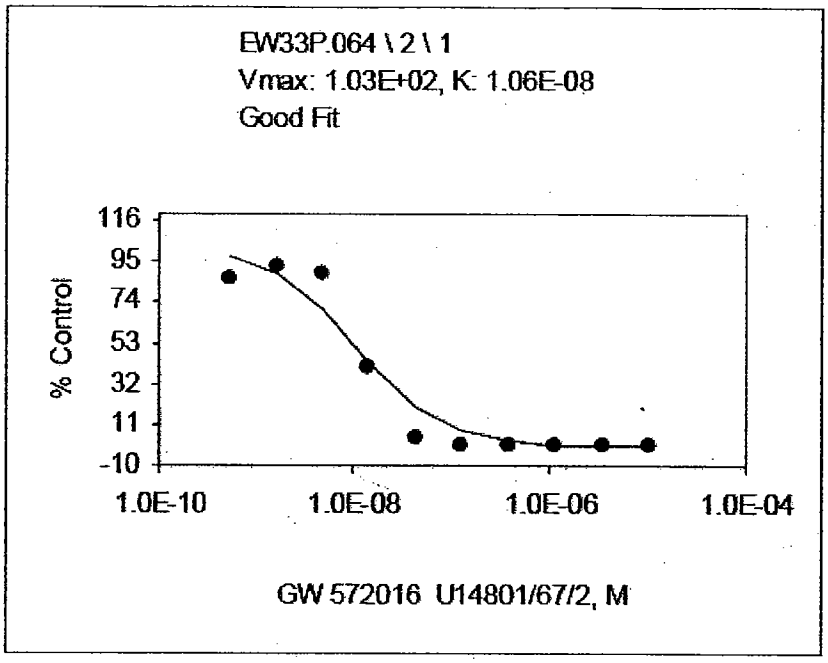

[Figure excerpted from sponsor]

RD2006/00999/00: A unique structure for epidermal growth factor bound to GW572016 (lapatinib): Relationships among protein conformation, inhibitor off-rate, and receptor activity in tumor cells

This study was undertaken to better understand why previous experiments have shown that with a variety of substituted quinazoline compounds, GW572016 included, the degree of inhibition of purified receptors did not necessarily equate to the degree of inhibition of intact cells. This experiment was designed to examine the inhibitor potency, ErbB receptor selectivity and inhibitor-enzyme dissociation rate of GW572016. Comparison of the inhibitory action of GW572016 is made to other 4-anilinoquinazoline compounds, such as ZD-1839 (Iresssa®), OSI-774 (Tarceva®), and —

The table below shows the results of studies evaluating enzyme inhibition using a purified enzyme assay system consisting of the recombinant human intracellular domain of each catalytically active ErbB family member. The results show the inhibition of ErbB2 and EGFR by GW572016 at nanomolar levels.

Table 1 ErbB Enzyme Inhibition by Compounds in Clinical Development

Compound	EGFR	ErbB-2	ErbB-4
			$^a = K_i^{app}$, $^b = IC_{50}$, $^c = cK_i^{app}$ (nM)
GW572016 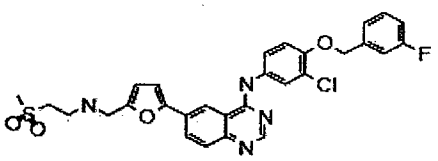	3.0 ± 0.2[a]	13 ± 1[a]	347 ± 16[c]
ZD 1839 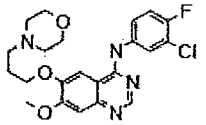	0.40 ± 0.1[a]	870 ± 90[a]	1130 ± 370[c]
OSI-774 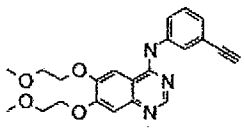	0.7 ± 0.1[a]	1000 ± 100[a]	1530 ± 270[c]

The method for enzyme assays, experimental design for potency estimation, and data analysis procedures were conducted as described in Experimental Procedures. The estimates of inhibitor affinity differ according to the mode of inhibition and potency of the particular result. K_i^{app} values were determined to assess tight-binding inhibition (IC_{50} < 500 nM). Calculated K_i^{app} values (cK_i^{app}) are given for inhibiton that yielded an initial IC_{50} > 1000 nM

[Table excerpted from sponsor]

An enzyme-reactivation procedure was used to study the inhibitor off-rate of GW572016 to further examine the fact that the IC_{50} as a function of time indicated that GW572016 exhibits time-dependant behavior. EGFR and inhibitor were incubated for 30 minutes to allow formation of an enzyme-inhibitor complex. The complex was then diluted into a reaction mixture containing a high ATP concentration and the phosphorylated product was evaluated as a function of time. In this assay, the change in the rate of product formation is a function of dissociation of the enzyme-inhibitor complex. In the graph below, the open circles represent GW572016 while the filled circle represents phosphorylation of EGFR with no pre-incubation with any inhibitor. The other points represent OSI-774 and ZD-1839, showing that the rate of formation of the phosphorylated product is the same regardless of the presence of OSI-774 or ZD-1839, indicating a rapid off-rate of the EGFR-OSI-774 and EGFR-Iressa complexes. The enzyme activity in the assay using GW572016 recovered much slower than when OSI-774 or ZD-1839 were present, indicative of a much slower off-rate.

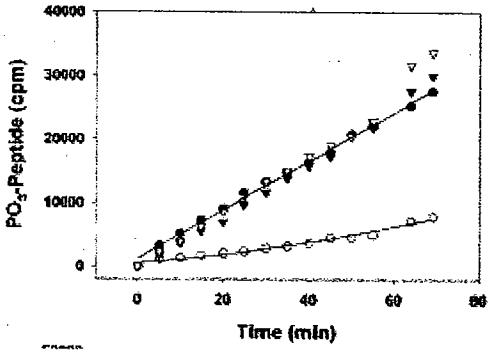

[Figure excerpted from sponsor]

The final graph shows a comparison of the results for EGFR (triangles) and ErbB-2 (circles) with GW572016. Again the open symbols represent GW572016 pre-incubation and the filled symbols represent no inhibitor pre-incubation. Similar results were seen with both enzymes.

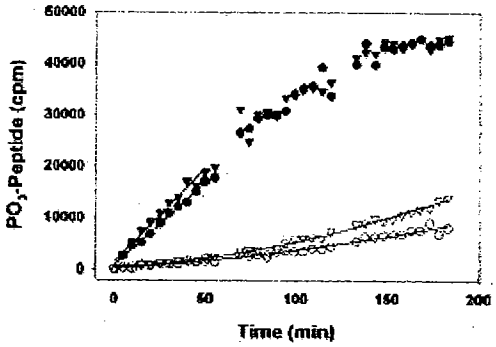

[Figure excerpted from sponsor]

The recovery of receptor phosphorylation after inhibitor washout was used to examine the relationship between recovery of autophosphorylation and the dissociation rate of the inhibitors. HN5 cells that naturally over-express EGFR were treated with either GW572016, OSI-774or ZD-1839, the inhibitor-containing media removed, cells rinsed extensively and fresh media with no inhibitor present added. Recovery of receptor tyrosine phosphorylation as a function of time is presented in the figure below. At 96 hrs the GW572016-treated cells had only recovered 15% of the control levels of tyrosine phosphorylated EGFR. It is speculated that the increased duration of suppression of ErbB receptor activity by GW572016 as compared to OSI-774 and ZD-1839 could be due to the slow inhibitor dissociation rate of GW572016.

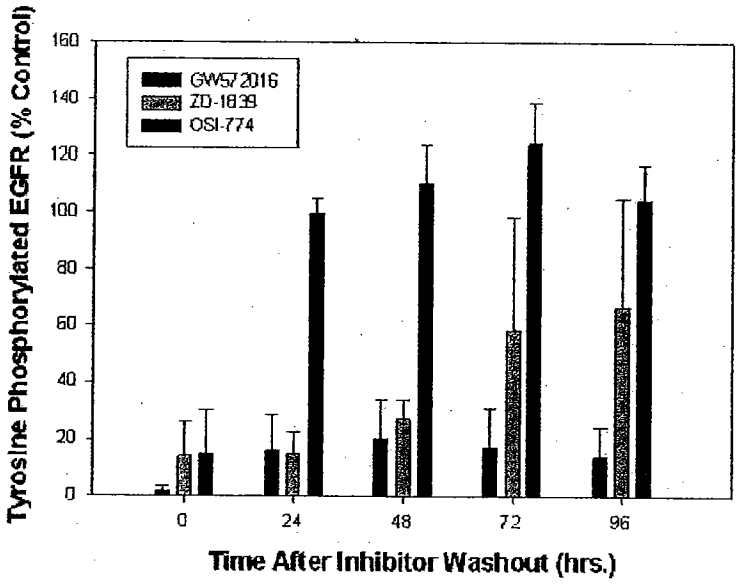

[Figure excerpted from sponsor]

To further examine why the dissociation rates of the GW572016-EGFR complex and the OSI-774-EGFR complex were so different the binding mode of GW572016 was evaluated by looking at the crystal structure of EGFR bound to the inhibitor. GW572016 binds in the ATP-binding cleft similarly to other kinase-quinazoline crystal structures. However when compared to the OSI-774-EGFR structure, the GW572016-EGFR complex differs in several ways. The shape of the ATP binding site, the position of the C helix, the conformations of the C-terminal tail and activation loop and the hydrogen bonding pattern with the quinazoline ring of the inhibitors are all ways in which the two complexes appear to differ. These results indicate that GW572016 appears to target an inactive form of the enzyme while OSI-774 targets an active one. This may account for the slow off-rate seen with GW572016. It should be noted that the structures for EGFR/GW572016 and EGFR/OSI-774 were derived from crystals obtained from different methods.

RR2000/00019/01: GW572016B is a highly selective inhibitor of epidermal growth factor receptor and ErbB-2 tyrosine kinase activities

The ability of GW572016 to inhibit a variety of protein kinases was examined. Included in the assay were the other active ErbB family member, ErbB-4 and other members of major classes of protein kinases (receptor tyrosine kinases, cytoplasmic tyrosine kinases, cell division cycle kinases (CDKs), MAP kinases, protein kinase C and other serine threonine kinases).

IC_{50} and % inhibition values were determined for the inhibition by GW572016 of 16 other kinases, excluding the EGFR and ErbB-2 enzymes. A single concentration of GW572016 was tested for its % inhibition relative to an uninhibited control and the results are presented below. The table shows that GW572016 did not inhibit any of these protein kinases at a level greater than 50% relative to control.

Enzyme	Concentration (μM)	% Inhibition
CDK-2/Cyclin A	10	-10.15
CDK-4/Cyclin A	10	41.46
GSK-3	13	10.95
IKK-2	1.5	16.09
Raf/MEK/ERK	6	11.30
P38	2	7.84
PDHK-4	11	17.01
PLK	10	4.13
TIE-2	7	15.55
VEGFR-2	7	6.43
Z-PKC	10	-13.48
cFMS	10	0.40
cSrc	3.75	31.00

[Table excerpted from sponsor]

Additional experiments were performed in a dose-response study with a subset of the protein kinases and including ErbB-4. The table below shows that GW572016 inhibits ErbB-4 with an IC_{50} of 360 nM, as opposed to the IC_{50} of 9 and 10 nM seen with ErbB-2 and EGFR, respectively. GW572016 had an IC_{50} of 3.5 μM for the inhibition of cSrc, a member of the non-receptor tyrosine kinase family.

Enzyme	IC_{50} (μM)
ErbB-4	0.36
CDK-4/Cyclin A	> 10
P38	> 10
VEGFR-2	> 10
Zap70	> 10
Lck	> 10
cSrc	3.5

[Table excerpted from sponsor]

Drug activity related to proposed indication:
RH2001/00009/01: The effects of GW572016 on the phosphorylation state of epidermal growth factor receptor, ErB-2, AKT and p42/44 ERK in the HN5 and BT474 cell lines

The EGFR over-expressing HN5 cell line and the ErbB-2 over-expressing cell line BT474 were used in a study to examine the ability of GW572016 to inhibit the phosphorylation of EGFR, ErbB-2, AKT, ERK 1 and ERK 2. The table below shows that equivalent inhibition of EGFR and ErbB-2 was seen between the two cell lines, regardless of their levels of over-expression of the enzymes

Cell line[1]	Immunoprecipitated[2] Receptor	Phosphotyrosine inhibition[3] (IC_{50}, μM)
BT474	EGFR	0.17 +/- 0.03
	ErbB-2	0.08+/- 0.02
HN5	EGFR	0.21 +/- 0.06
	ErbB2	0. 06 +/- 0.03

[Table excerpted from sponsor]

Western blot analyses showed that GW572016 inhibited AKT phosphorylation to a much greater extent in the cell line that over-expresses ErbB-2 and inhibited ERK 1/2 phosphorylation more in the cell line over-expressing EGFR. GW572016 inhibited both AKT and ERK 1/2 in a dose-dependant manner.

RH2006/00069/01: Regulation of survivin protein by GW572016

Over-expression of ErbB-2 in breast cancer is associated with resistance to chemo/hormone therapy and may be an indicator of a poor outcome. Aberrant regulation of survivin, the human anti-apoptosis protein, may also be an indicator of a poor outcome. Two ErbB-2 over-expressing breast cancer cell lines were used to examine the effects of GW572016 on ErbB-2 inhibition and on survivin levels. The figure below shows that GW572016, but not trastuzumab, down-regulated survivin steady-state protein, and in turn increased tumor cell apoptosis as depicted by the increase in annexin V staining.

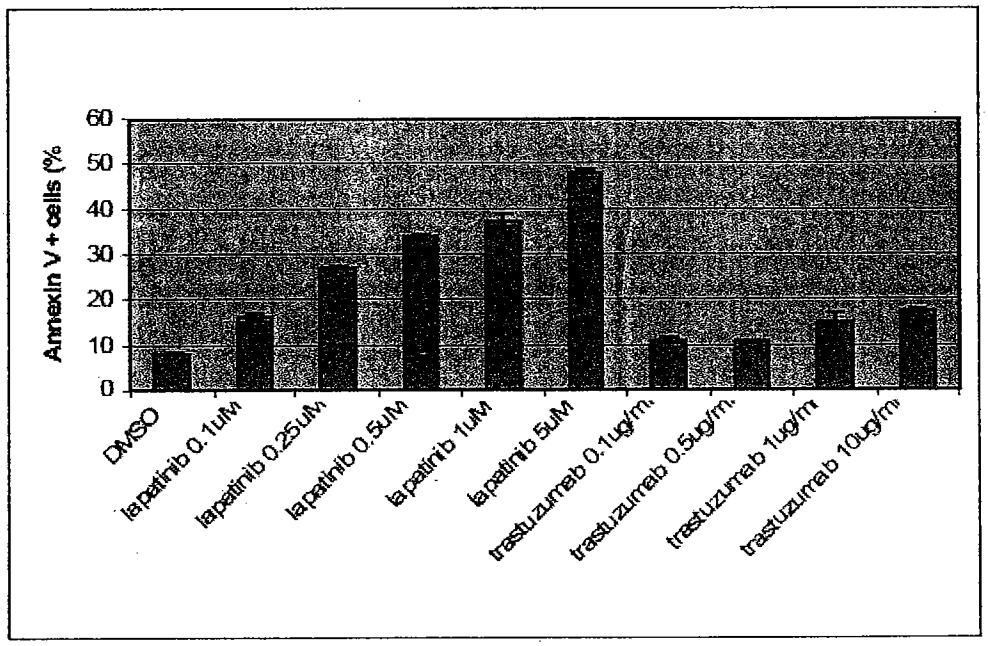

[Figure excerpted from sponsor]

RR2000/00003/01: The effects of GW572016 on the growth of human normal and transformed cell lines

Four human transformed cell lines that over-express either EGFR or erbB-2 were used to compare the effects of GW572016 on cell growth inhibition with the effect of GW572016 on normal human foreskin fibroblasts (HFF). The tumor cell lines were HN5 (human squamous cell head and neck cancer), BT474 (human breast carcinoma), N87 (human gastric carcinoma), and HB4a c5.2 (erbB-2 transfected breast epithelial cells). The following graph shows the cell growth, as measured by the methylene blue growth inhibition assay, of the four tumor cells and the normal cell line after incubation for 72 hrs with GW572016. Greater inhibition of cell growth is seen in the cell lines known to over express either EGFR or erbB-2 than in the normal cell line.

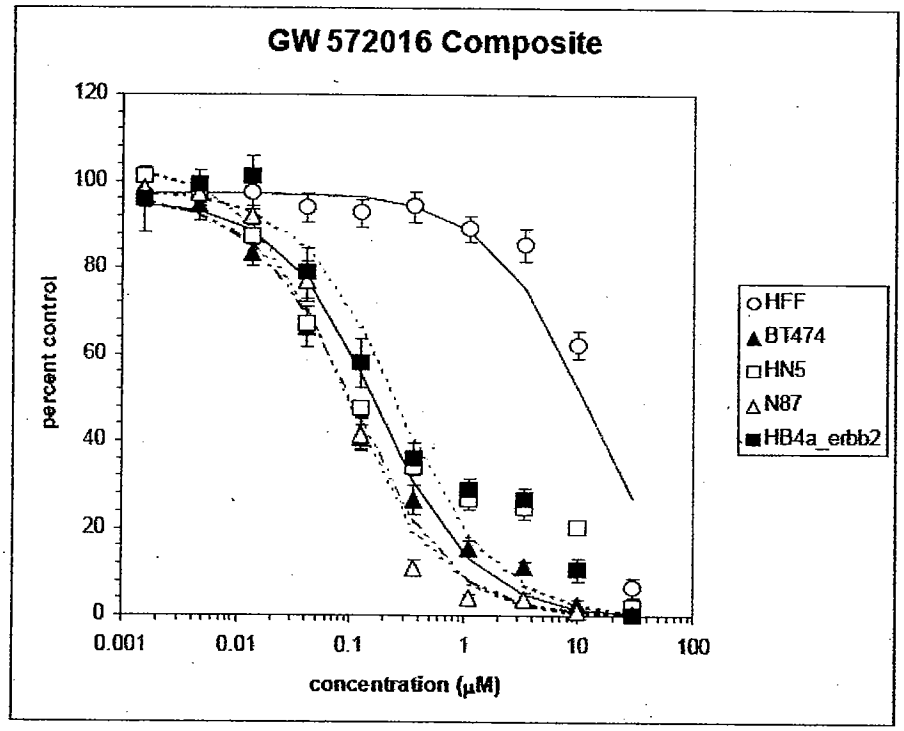

[Figure excerpted from sponsor]

APPEARS THIS WAY
ON ORIGINAL

The IC_{50} for GW572016-induced growth inhibition in these cell lines is presented in the table below. The IC_{50} for GW572016 in the normal cell line is 59-136 fold higher than the IC_{50} for GW572016 in the over-expressing cell lines.

Cell line	IC_{50} (ng/ml)	IC_{50} (μM)
HFF	8040 +/- 916	12.30 +/- 1.40
BT474	75.9 +/- 18.3	0.116 +/- 0.028
HN5	95.5 +/- 21.6	0.146 +/- 0.033
N87	58.9 +/- 9.8	0.090 +/- 0.015
HB4a c5.2	136 +/- 22	0.210 +/- 0.033

[Table excerpted from sponsor]

Additional studies were conducted to determine if GW572016 could yield irreversible growth inhibition. Several cell lines were incubated with GW572016 for 3 days and the following day the medium was replaced with GW572016-free medium and the cells were allowed to grow for three weeks with no further GW572016 exposure. The methylene blue assay was used at time points from the removal of GW572016 and throughout the total of 18 days. As the figure below shows, in each of the tested cell lines, there was a concentration of GW572016 where further outgrowth of cells did not occur in the time frame of the experiment. The concentrations where this occurred were at levels at least 4-fold higher than previously determined IC_{90} concentrations for GW572016 in the respective cell lines.

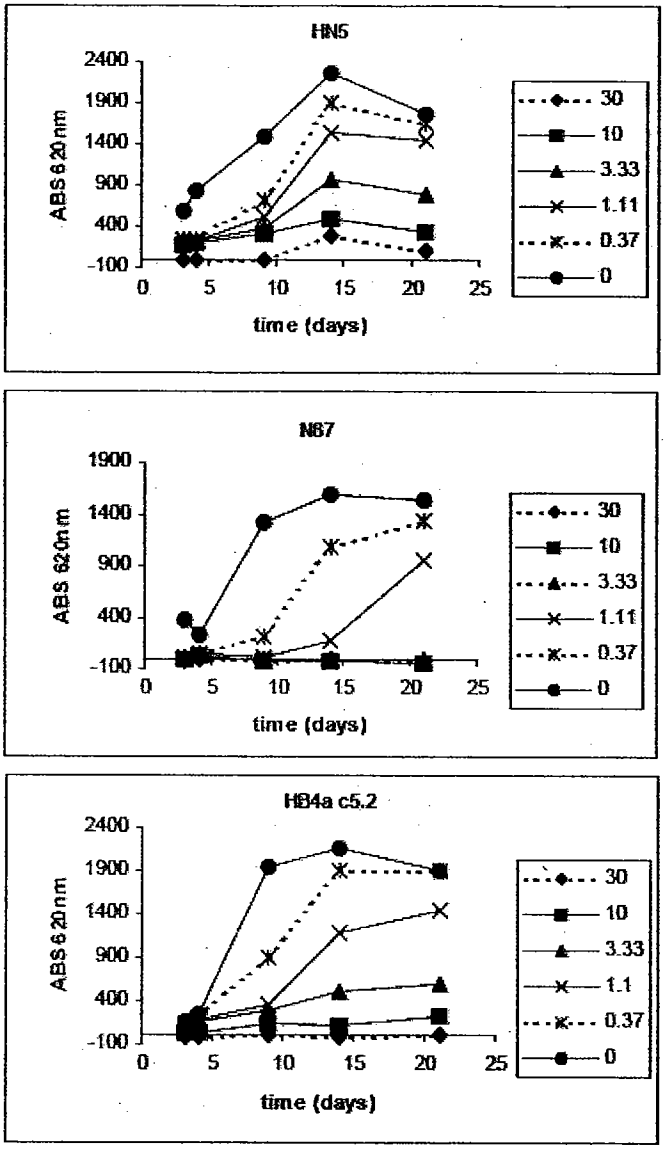

[Figure excerpted from sponsor]

RH2003/00020/00: The effects of compound dilution protocol and salt form on the reported cellular growth inhibition properties of GW572016

This study was conducted to verify that there was no change in the growth inhibition by GW572016 when the drug development changed from — ., GW572016B, to the ditosylate salt, GW572016F, the form used in the clinical formulation. Previous cell growth inhibition studies not only used GW572016B, but also used a dilution method that likely led to drug precipitate that may have affected the actual drug concentration used in the assays. This study compared both the two formulations as well as two methods for diluting the formulations, in aqueous media or DMSO. The table below shows that

although the IC_{50} values differ for the purpose of reporting the specific values for the relevant drug formulation, the change to the ditosylate salt did not alter the values significantly.

Table 1 IC_{50} values for GW572016

Cell Line	GW572016F IC_{50} (μM)		GW572016B IC_{50} (μM)	
	Growth Media Dilutions (n = 4)	DMSO Dilutions (n ≥ 12)	Growth Media Dilutions[1]	DMSO Dilutions (n = 6)
HFF	7.52±0.20	6.45±0.78	12.30±1.40	10.03±0.057
BT474	0.048±0.003	0.025±0.004	0.116±0.028	0.027±0.005
HN5	0.089±0.010	0.029±0.005	0.146±0.033	0.054±0.009
N87	0.057±0.010	0.028±0.002	0.090±0.015	0.036±0.006
HB4a c5.2	0.124±0.047	0.027±0.003	0.210±0.033	0.032±0.011[3]
HB4a r4.2	5.76±0.32	5.73±0.26	8.32±0.36[2]	5.69±0.51

1. Previously reported for GW572016B (GSK Document Number RR2000/00003/00) except where noted (**).
2. Previously unreported data for GW572016B, n = 6.
3. n = 4.

[Table excerpted from sponsor]

APPEARS THIS WAY
ON ORIGINAL

RC2006/00095/00: Assessment of tumor cell growth inhibition by the combination of lapatinib ditosylate (GW572016F) and 5-fluorouracil (5-FU)

This study was conducted using four cell lines from lung (A549, NCI-H1299), colon (COLO205) and breast (MDA-MB-468) tumor tissues. These cell lines have low levels of ErbB-2 expression and therefore have a limited response to lapatinb. Dose response curves of cell growth after treatment with the drugs alone or in combination showed that the addition of lapatinib to 5-FU did not worsen the growth inhibition and in several experiments, particularly with A549 and COLO205 the addition of lapatinib improved the response. The graphs below show the dose-response curves for cell growth inhibition for both drugs alone and the combination.

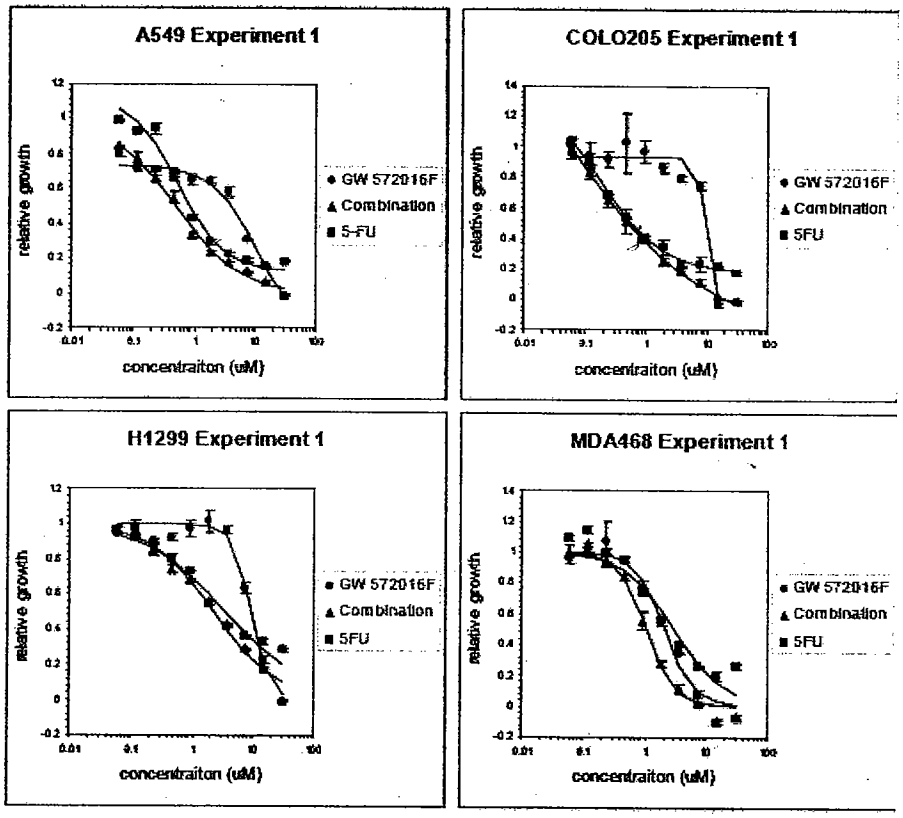

[Figure excerpted from sponsor]

The data from this study were used to calculate a combination index value (CI), a method of analysis by Chou and Talalay, though this is not a method that was validated by the Sponsor for analyses with GW572016. The Chou and Talalay analysis yields a CI value for GW572016 in combination with 5-FU and the CI is used to characterize drug combinations and their interactions as being synergistic (CI<1), antagonistic (CI>1) or additive (CI~1). The average CI value for lapatinb and 5FU combined in this study range from 0.84 to 1.14, indicating an approximately additive effect of the combination.

Table 1 **Mutually non-exclusive CI values generated at the IC_{50} by a modified method of Chou and Talalay.**

Cell Line	Individual CI Values	Average CI Value +/- 95% Confidence Interval
A549	0.78, 0.89	0.84 +/- 0.11
COLO205	0.99, 0.90	0.95 +/- 0.09
H1299	1.02, 1.26	1.14 +/- 0.24
MDA468	1.04, 1.15	1.10 +/- 0.11

RR2000/00021/02: Antitumor activity of GW572016B in the ErbB-2 positive BT474 human breast cancer xenograft

SCID mice transfected with the erbB-2 over-expressing human ductal breast carcinoma BT474. Mice were dosed BID for 21 days with 0, 30 or 100 mg/kg and tumor growth inhibition was measured. The results showed that the 100 mg/kg dose led to an average of 94 ± 18% growth inhibition, with less inhibition seen in the 20 mg/kg mice (42 ± 35%). Tumor regressions were noted in the 100 mg/kg group but not the 30 mg/kg dose group. The graph below shows the comparison of the tumor size in the control mice to the tumors in the mice treated with two doses of GW572016 BID for 21 days.

Figure 4 Inhibition Of BT474 Growth By GW572016B

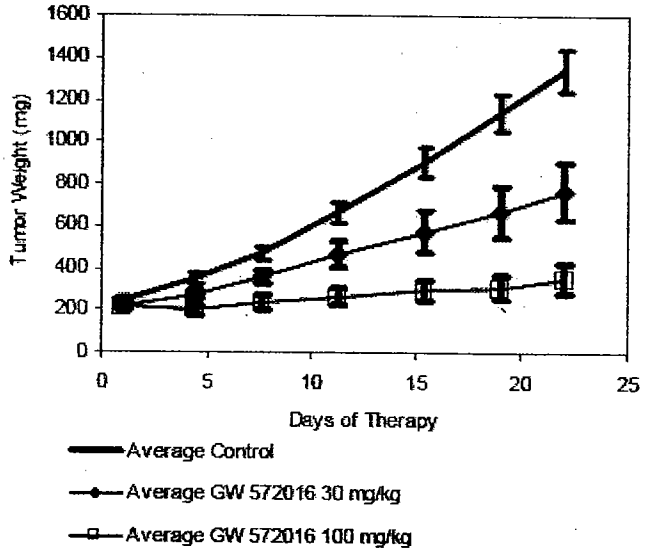

[Figure excerpted from sponsor]

Tumors in additional mice dosed with 100 mg/kg BID were excised following a 5-day dosing regimen and the level of erbB-2 tyrosine phosphorylation (P-Tyr), as a measure of enzyme activity, was determined by immunoblotting techniques. The level of erbB-2 P-Tyr was reduced 93 ± 3% in the tumors of the GW572016-treated mice when compared to control. The Western blots for P-Tyr in the control mice (A) and the 100 mg/kg BID x 5 GW572016 mice (B) are shown in the figure below (N=3 mice).

Figure 5 Effect Of GW572016B Upon erbB-2 P-Tyr

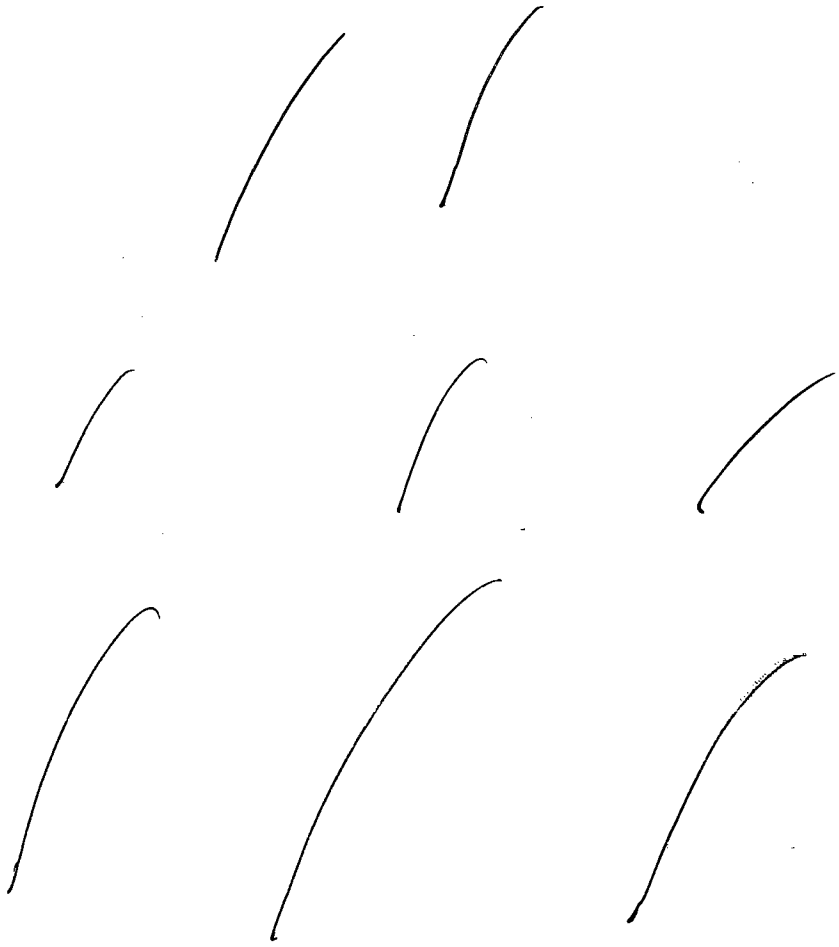

2.6.2.3 Secondary pharmacodynamics

RR2000/00069/00: Secondary pharmacological evaluation of the dual ErbB-2 tyrosine kinase inhibitor GW572016B in radioligand binding and isolated tissues assays.

Radioligand binding and isolated tissues assays were used to assay the potential for GW572016 to interact with common pharmacological receptor and ion channel sites. GW572016 is a dual EGFR/erbB2 tyrosine kinase inhibitor.

The ability of a concentration of 30 μM of GW572016 to inhibit or enhance the binding of a radioligand to its specific binding site was studied in a screen that used 38 binding sites and the appropriate radioligand. Significant displacement of the radioligand (≥ 50%) was seen at only five of the binding sites: sigma, sodium channel, noradrenergic, L-type calcium channel and dopamine transporter.

Binding Site	Percent Inhibition of Binding
Adrenergic NE transporter (human recombinant)	54
Calcium channel, L-type (rat cortex)	60
Dopamine transporter (human recombinant)	89
Sigma, non-selective (guinea pig brain)	109
Sodium channel, site 2 (rat brain)	107

Binding at these sites were further characterized using a range of drug concentrations (100 nM to 100 μM) to obtain IC_{50} values. Reference agents appropriate for each binding site were also tested. The sponsor's table below presents the results of this further elucidation of the binding of GW572016 at several binding sites. Inhibition of these binding sites occurred at IC_{50} concentrations in the 1-26 μM range, while the reference agents had IC_{50} values ranging from 0.7 nM to 0.9 μM. Previous studies have shown that GW572016 has an IC_{50} value at its proposed site of action (EGFR/erbB2) in the 10nM range.

Table 4 **Binding characteristics of GW572016B and reference agents to various sites in radioligand binding assays**

Agent	Site	IC_{50} (M)	% Maximum Inhibition[a]
GW572016B	Sigma Receptor (Non-selective)	1.1×10^{-6}	105 ± 0.4
Haloperidol	Sigma Receptor (Non-selective)	3.8×10^{-9}	89 ± 2.3
GW572016B	Sodium Channel, Site 2	2.6×10^{-6}	117 ± 1.7
Dibucaine	Sodium Channel, Site 2	8.7×10^{-7}	104 ± 1.3
GW572016B	Dopamine Transporter	9.0×10^{-6}	68 ± 1.3
GBR-12909[b]	Dopamine Transporter	1.7×10^{-9}	74 ± 0.0
GW572016B	Calcium Channel, Type L	1.8×10^{-5}	63 ± 1.7
Nitrendipine	Calcium Channel, Type L	7.2×10^{-10}	89 ± 1.3
GW572016B	Noradrenergic Transporter	2.6×10^{-5}	53 ± 0.2
Desipramine	Noradrenergic Transporter	9.3×10^{-10}	86 ± 0.9

[a] Expressed as a percentage of maximum displacement of binding of the radioligand, mean ± SEM of 3 determinations. The percent of maximum inhibition values obtained with GW572016B represent concentrations of 30-100 µM.
[b] GBR-12909=1-[2[bis(4-fluorophenyl)methoxy]ethyl]-4-[3-phenylpropyl]piperazine diHCl.

[Table excerpted from sponsor]

Additional studies were conducted to examine the potential of GW572016 to interact at the sigma and sodium channels, given the low (<5 µM) IC_{50} values obtained. The functional activity of GW572016 at these sites was tested using up to 100 µM of drug and testing for functional agonist or antagonist activity at the sigma receptor or sodium channel using the field-stimulated guinea pig vas deferens and left atrial preparations, respectively. In the guinea pig field-stimulated vas deferens preparation the sigma receptor agonist (+)-3-PP (100 µM) produced a 100% increase in the amplitude of the neurogenic twitch contractile activity within 5 minutes. The sigma receptor antagonist rimcazole (30 µM) almost completely (97%) abolished the (+)-3-PP effect on twitch contractions. GW572016 alone had little or no effect on increasing the amplitude of the neurogenic twitch contractile activity and it had only a minor non-significant effect on inhibition of the (+)-3-PP-induced twitch contractions.

Table 5 Effects of GW572016B and reference agents in isolated guinea pig vas deferens assay for sigma receptor activity

Compound	Conc.	N	Agonism (%)	Antagonism (%)
Vehicle (DMSO)	0.1%	2	0	0
(+)-3-PPP	100 µM	2	100	ND
Rimcazole	30 µM	2	0	97
GW572016B	30 µM	4	-2 ± 1	0 ± 0
GW572016B	100 µM	4	1 ± 3	23 ± 5

A strip of guinea pig vas deferens was placed under 1 g tension in a 10 ml bath containing oxygenated Kreb's solution with pyrilamine maleate (0.25 nM) and choline chloride (0.2 µM) pH 7.4 at 32°C. Test substance-induced isometrically recorded contractile response within 5 minutes indicated possible sigma agonist activity. At a test substance concentration where no significant agonist activity was seen (<50% relative to the 100 µM (+)-3-PPP-induced contractile response), ability to reduce the (+)-3-PPP-induced response indicated antagonist activity. ND: Not determined because significant agonist activity was observed. (+)-3-PPP=(+)-3-(3-hydroxyphenyl)-N-propylpiperidine.

[Table excerpted from sponsor]

In the guinea pig left atrial preparation the sodium channel blocker, dibucaine, was used as the reference material and a concentration of 3 µM produced a nearly complete blockade of the paced atrial chronicity. GW572016 at concentrations as high as 100 µ M did not show sodium channel agonist or antagonist activity. GW572016 did not induce negative chronotropy by 50% or more within 30 minutes, as would a sodium channel antagonist. A sodium channel agonist would reduce the dibucaine-induced response in the left atrial assay and GW572016 also did not do this.

APPEARS THIS WAY
ON ORIGINAL

Table 6 Effects of GW572016B and reference agents in isolated field-stimulated guinea pig left atrial assay for sodium channel activity

Compound	Conc.	N	Agonism (%)	Antagonism (%)
Vehicle (DMSO)	0.1%	2	0	0
Dibucaine	3 µM	2	0	100
GW572016B	30 µM	4	0	0 ± 0
GW572016B	100 µM	4	0	0 ± 0

A guinea pig left atria was placed under 1 g tension and subjected to field stimulation in a 10 ml bath containing oxygenated McEwen's solution pH 7.4 at 32°C. Test substance-induced isometrically recorded negative chronotropy by 50 percent or more (≥50%) within 30 minutes indicated sodium channel antagonist activity. At a concentration where no significant antagonist activity was seen (<50% relative to 3 µM dibucaine-induced negative chronotropy response), ability to reduce the dibucaine-induced response indicated agonist activity.

[Table excerpted from sponsor]

In summary, although there was evidence that GW572016 bound to the sigma and sodium channel receptors at IC_{50} values in the 1-3 µM range, functional assays with guinea pig vas deferens and left atrial preparations did not show any functional activity, agonism or antagonism, by GW572016.

2.6.2.4 Safety pharmacology

Neurological effects:
RD2000/00236/00: GW572016F: Safety pharmacology study of overt central and peripheral pharmacodynamic effects following single-dose oral administration in conscious female Wistar Han rats.

Rats were administered a single dose of 50, 150 or 500 mg/kg of GW572016F by oral gavage (N=3/dose) in this GLP study. After administration, rats were placed in clear chambers where each drug-treated rat was observed in comparison to a time-matched vehicle-treated rat. Rats were monitored for changes in behavior, skeletal muscle tone, reflexes and overt autonomic, gastrointestinal and neurological effects. The time period of observation was the first 30 minutes after dosing, then at 2, 4 and 7.5 hours post-administration. A final observation was conducted at 24 hrs after dosing, at which time the rats were euthanized. No deaths occurred during the study and no differences in the overt pharmacodynamic effects based on the aforementioned observational data were seen.

RD2000/00237/00: GW572016F: Safety pharmacology study of overt central and peripheral pharmacodynamic effects following single-dose oral administration in conscious beagle dog.

Conscious male dogs were administered a single oral dose of 50, 150 or 500 mg/kg of GW572016F by gelatin capsule (N=2/dose) in this GLP study. After administration, dogs were returned to their cages where they were monitored by close-circuit TV and compared with vehicle control dogs. Dogs were monitored for changes in behavior, skeletal muscle tone, reflexes and overt autonomic, gastrointestinal and neurological effects. The time period of observation was the first 60 minutes after dosing, then at 2, 3 and 4 hrs. A final observation was conducted at 24 hrs after dosing, and then dogs were checked twice-daily for any morbidity for the next 7 days. Additionally, heart rate, respiration rate and rectal body temperatures were collected twice prior to dosing and then immediately after the 1, 3, 4, and 24 hr observation periods. No deaths occurred during the study and no differences in any of the parameters were seen.

Cardiovascular effects:

WD2000/00426/00: GW572016B (ErbB-2 inhibitor) Safety pharmacology: cardiovascular effects following acute intraduodenal administration in anaesthetized Wistar Han rats.

Arterial blood pressure, heart rate, ECG and tracheal inflation pressure were measured in anesthetized rats following single exposure to vehicle, 100 or 300 mg/kg of GW572016 administered via an intraduodenal catheter in a non-GLP study. Measurements were taken 1, 2, 5, 10, 15, 30, 45, 60, 75, 90, 105 and 120 minutes after drug administration. Two rats were tested with the vehicle and 3 rats at each dose of GW572016. No effects of GW572016 were seen in tracheal inflation pressure. Both doses of GW572016 led to slight, transient decreases in arterial pressure and heart rate, never exceeding a 15% change from baseline measurement. One rat dosed with 100 mg/kg of GW572016 exhibited premature ventricular contractions for approximately 65 minutes, from 7-72 minutes post-administration. Neither of the other rats in this dose group or any of the rights in the higher dose group had a similar response. Overall, the ECG waveform and the PR, QT, QTcB, QTcF, and QRS intervals were not significantly affected by GW572016 administration. The single rat with premature ventricular contractions, while not definitive of a cardiovascular effect of GW572016, it suggests that a potential should not be ruled out.

RD2000/00143/01: GW572016F: Evaluation of cardiovascular (hemodynamic) functions following acute oral administration to conscious telemetered male Wistar Han rats.

Heart rate, arterial pressure, body temperature, and ECG were measured in four male rats implanted with telemetry transducers in a GLP study. The rats were exposed to all dose groups, with a washout period of at least seven half-lives of the GW572016. Rats were administered 50, 150 and 500 mg/kg of GW572016 and the vehicle by oral gavage. Data were collected for 24 hrs before any drug administration to obtain baseline information

and also beginning 30 minutes prior to dosing after which waveforms were recorded continuously for 24 hrs after drug administration. Blood pressure and heart rate were calculated every one minute interval from these waveforms. No effect of GW572016 administration were seen on heart rate, body temperature, mean arterial pressure, diastolic arterial pressure, systolic arterial pressure or ECG waveforms under the conditions of this study.

RD2000/01107/00: GW572016F: Evaluation of cardiovascular (hemodynamic) functions following acute oral capsule administration to conscious telemetered male beagle dogs.

Heart rate, arterial pressure, body temperature, and ECG were measured in four male beagle dogs implanted with telemetry transducers in a GLP study. The dogs were exposed to all dose groups, with a washout period of at least seven half-lives of the GW572016. Dogs were orally administered 50, 150 and 500 mg/kg of GW572016 and the vehicle by gelatin capsule. Data were collected for 24 hrs before any drug administration to obtain baseline information and also beginning 30 minutes prior to dosing after which waveforms were recorded continuously for 24 hrs after drug administration. ECG tracings were also evaluated by a veterinary cardiologist at periodic intervals. Increases in mean systolic, diastolic and arterial pressures were seen with 150 and 500 mg/kg GW572016 doses during the 10-14 hr or 6-14 hr timeframes, respectively. The pressures were, however, within normal physiological ranges and the drug effect was likely due to the decrease in pressure seen after vehicle administration. An ANOVA indicated a significant group effect over the 24-hr period in heart rate and mean arterial pressure after 500 mg/kg of GW572016 and in mean systolic arterial pressure after all 3 GW572016 doses, in a dose-response fashion. Additional statistics showed no group by time interaction and no specific time intervals over the 24 hrs was significant. One dog had 3 ventricular extrasystoles at 5 hrs after 50 mg/kg GW572016 administration, which is approximately 1 hr after the Tmax. All other dogs had normal ECG recordings and while GW572016 can not be ruled out as the cause of the ventricular extrasystoles, it is unlikely.

RR2000/00076/00: The effects of GW572016F on canine Purkinje fiber action potentials.

Adult beagle dogs were deeply anesthetized and a right thoracotomy performed to remove the heart in a non-GLP study. Purkinje fibers were dissected from the ventricles and isolated in a bath where transmembrane potentials were recorded after a 45-60 minute period for tissue equilibration. Four concentrations of GW572016F were tested (0.08, 0.8, 2.4 and 4.0 µg/mL) along with the control of physiological salt solution (PSS). Additionally, the drug vehicle (sulfobutylether (beta) cyclodextrin) was tested as it was required to get GW572016F into solution. A positive control, the class III antiarrhythmic (±)-sotalol, was used to confirm the assay. The Purkinje fibers were stimulated at rates of 1 and 3 Hz. The vehicle, when added to the PSS, increased the action potential duration at 60% and 90% repolarization (APD_{60} and APD_{90}) when compared to PSS alone. The positive control significantly increased APD_{60} and APD_{90} when compared to the vehicle

exposure. But when the evoked action potentials recorded from the fibers in any of the four concentrations of GW572016F were compared to the vehicle, there was no significant difference. GW572016F had no effect, minus the effect of the vehicle, on the duration of the action potential under the conditions tested. However, analysis of the solutions indicated that the highest GW572016F concentration tested was approximately 2.6 µg/mL rather than 4.0 µg/mL.

Pulmonary effects:
RD2000/00144/00: GW572016F: Airway resistance and dynamic lung compliance in male guinea pigs.

A GLP study was conducted in four male guinea pigs/dose with GW572016 doses of 50, 150 and 500 mg/kg and a control group. Dynamic lung compliance, airway resistance and respiratory rates were recorded or calculated from guinea pigs anesthetized at least 30 minutes prior to the estimated T_{max} following drug administration. Pulmonary function studies were conducted using a whole-body plethysmograph. Results showed decreases in dynamic lung compliance and respiratory rates and increases in airway resistance when drug treated groups were compared to controls. The results were not dose-related or consistent across the 30 minutes that data were collected. The changes were also not statistically significant. These results suggest that GW572016 does not have an effect on pulmonary activity in the guinea pig under the design of this study.

Renal effects:
No studies conducted

Gastrointestinal effects:
No studies conducted

Abuse liability:
No studies conducted

Other:
None

2.6.2.5 Pharmacodynamic drug interactions
No studies conducted

2.6.3 PHARMACOLOGY TABULATED SUMMARY

Summary of the Effectiveness of GW572016 In Biological Assays – IC_{50} Values	
Assay Systems	**IC_{50} ng/ml**
Inhibition of purified EGFR – baculovirus expression	10.8
Inhibition of Purified erbB-2 – baculovirus expression	9.2
Inhibition of purified EGFR – recombinant human intracellular domain	3.0
Inhibition of purified erbB-2 – recombinant human intracellular domain	13
Inhibition of cell growth – BT474 tumor cell line	116
Inhibition of cell growth – HN5 tumor cell line	146
Inhibition of cell growth – N87 tumor cell line	90
Inhibition of cell growth – HB4a c5.2 tumor cell line	210

2.6.4 PHARMACOKINETICS/TOXICOKINETICS

2.6.4.1 Brief summary

The pharmacokinetic behavior of lapatinib was examined in all the non-clinical species tested for toxicity. As the doses increased in the animals, proportional increases were usually seen in AUC. In the rat, there was a definite gender difference in drug exposure, with higher AUCs in the female than the male. This correlated with the increased toxicity usually noted in female rats.

The metabolic profile of lapatinib is very similar across species; mouse, rat, dog, and human. The major metabolic pathway has been determined, with the O-dealkylation metabolite found in the feces, the major route of excretion. Additional metabolism included N-dealkylation and oxidation. Metabolism appears to involve the P450 isozymes CYP3A4 and CYP3A5.

2.6.4.2 Methods of Analysis

[see under individual study reviews]

2.6.4.3 Absorption

RD2000/00063/00: Single dose pharmacokinetics of GW572016F in male CD mice, Han Wistar rats and beagle dogs after intravenous and oral administration

Rats, mice and dogs were given oral and IV administrations of the ditosylate salt and the pharmacokinetics were determined. Oral bioavailability in the dog = 41.9%, the rat = 24.0% and the mouse = 50.0% at the dose of 10 mg/kg, with less bioavailability seen at the 2 mg/kg dose. In all three species the half-lives were longer after IV administration than oral.

Pharmacokinetic parameters of GW572016X in Male beagle Dogs (mean ± SD)							
Route/ Dose (mg/kg)	AUC_∞ (ng hr/mL)	C_{max} (ng/mL)	T_{max} (h)	$t_{½}$ (h)	CL (mL/min/kg)	V_{ss} (L/kg)	F
IV/10	14087 ± 3094	3793 ± 167	0.08	5.85 ± 0.17	12.2 ± 2.83	5.70 ± 1.03	–
PO/10	5916 ± 852	555 ± 15.1	4.00	3.27 ± 1.18	-	-	41.9 ± 6.06
PO/2	197 ± 127	24.9 ± 13.2	4.00	3.61 ± 0.95	-	-	6.97 ± 4.50

Pharmacokinetic parameters of GW572016X in Male Han Wistar rats (mean ± SD)							
Route/ Dose (mg/kg)	AUC_∞ (ng hr/mL)	C_{max} (ng/mL)	T_{max} (h)	$t_{½}$ (h)	CL (mL/min/kg)	V_{ss} (L/kg)	F
IV/10	3596 ± 924	4557 ± 1210	0.08	12.3 ±8.24	48.8 ± 14.3	6.16 ± 1.95	–
PO/10	861 ± 420	288 ± 224	0.50–1.00	3.91 ± 3.98	–	–	24.0 ± 11.6
PO/2	39.5 ± 26.1	17.8 ± 0.64	0.50–1.00	1.37 ± 0.96	–	–	5.50± 3.68

Pharmacokinetic parameters of GW572016X in Male CD Mice (mean ± SD)							
Route/ Dose (mg/kg)	AUC_∞ (ng hr/mL)	C_{max} (ng/mL)	T_{max} (h)	$t_{½}$ (h)	CL (mL/min/kg)	V_{ss} (L/kg)	F
IV/10	3469	942	0.50	5.69	48.0	9.55	-
PO/10	1735	504	0.50	1.99	-	-	50.0
PO/2	302	123	2.00	0.67	-	-	43.0

[Table excerpted from Sponsor]

RD2000/00696/00: Single and repeat dose pharmacokinetics of GW572016F in female CD-1 nude mice after oral administration for up to 14 days

Nude mice were dosed with 30 or 100 mg/kg of GW572016 either BID for 14-days continuously or as a single dose. AUC increased after single doses in a greater than proportional manner. Twice daily treatment resulted in a proportional increase in both C_{max} and AUC.

Parameter	30 mg/kg	30 mg/kg BID	100 mg/kg	100 mg/kg BID	Units
C_{max}:	3225	3727	8099	12646	ng/mL
T_{max}:	1	1	2	12	hr
AUC_t:	7541	47002	57840	178759	hr·ng/mL
AUC_{∞} :	8199	-	58783	-	hr·ng/mL
extrap.AUC :	8.03	-	1.60	-	%
$T_{½}$:	2.72	-	4.02	-	hr

[Table excerpted from Sponsor]

RD2000/00327/00: Pharmacokinetics of GW572016X following intravenous and oral administration of GW572016F to male rats

Male rats were administered 10 mg/kg GW572016 orally or IV and blood samples taken to measure pharmacokinetic parameters of GW572016. The pharmacokinetic parameters are presented in the table below and show an oral bioavailability in the rats of 28.7%.

Pharmacokinetic Parameters of Parent Compound									
Route	Dose (mg/kg)		$AUC_{0\rightarrow\infty}$ (ng*h/mL)	C_{max} (ng/mL)	T_{max} (h)	$t_{½}$ (h)	CL (mL/min/kg)	V_{ss} (mL/kg)	F
IV	10	Mean	8275	10496	0.03-0.5	3.11	22.9	1815	
		SD	2199	2061		1.68	5.36	535	
PO	10	Mean	2375	535	0.5-4	1.45			28.7%
		SD	1067	376		0.33			12.9%

n = 7

[Table excerpted from Sponsor]

RD2000/02336/00: Pharmacokinetics of GW572016X following oral administration of GW572016F and GW572016X to male Wistar Han rats

Pharmacokinetic parameters were measured after the free base compound GW572016X was administered to fasted rats or the ditosylate salt GW572016F was administered to fed or fasted rats at a dose of 10 mg/kg of the free base. Exposure levels were higher in the fasted rats than the fed, and when the fasted rats were given the salt form rather than the free base. Other pharmacokinetic parameters (C_{max}, T_{max}, $t_{1/2}$) were not affected by the formulation or the fasting.

	Pharmacokinetic Parameters of GW572016X in Male Wistar Han Rats							
Study Number[1]	Compound		AUC_{∞} (h*ng/mL)	C_{max} (ng/mL)	T_{max} (hr)	$t_{½}$ (hr)	Dose-Normalized[2] AUC	C_{max}
00AVV0002	GW572016F	Mean	2375	535	0.5-4	1.45	2293	516
(Fed)		SD	1067	376		0.33	1024	361
00APK0051	GW572016F	Mean	3730	621	1-6	1.35	4575	760
(Fasted)		SD	980	93.1		0.26	1268	120
00APK0051	GW572016X	Mean	2107	460	0.5-8	1.51	2235	487
(Fasted)		SD	816	273		0.68	885	288

n = 5 or 7

[1] Prior to dosing, the rats in study 00AVV0002 (Glaxo Wellcome report RD2000/00327/00) were allowed access to food and the rats in Study 00APK0051 (Glaxo Wellcome report RD2000/02336/00) were fasted.

[2] The AUC and C_{max} values were normalised to 10 mg/kg.

[Table excerpted from Sponsor]

APPEARS THIS WAY
ON ORIGINAL

RD2000/00321/00: Pharmacokinetics of GW572016X following intravenous and oral administration of GW572016F to male beagle dogs

Fasted dogs were administered single doses of GW572016 orally or intravenously and blood was taken for pharmacokinetic analysis. The findings are presented in the table below and show that oral bioavailability was 63.2%.

Pharmacokinetic Parameters of Parent Compound									
Route	Dose (mg/kg)		$AUC_{0\rightarrow\infty}$ (ng*h/mL)	C_{max} (ng/mL)	T_{max} (h)	$t_{½}$ (h)	CL (mL/min/kg)	V_{ss} (mL/kg)	F
IV	10	Mean	13111			4.63	14.6	5163	
		SD	4052			0.83	4.54	1515	
PO	10	Mean	8291	1016	4-6	2.92			63.2%
		SD	5560	578		0.95			42.4%

n = 6

[Table excerpted from Sponsor]

RD2000/02334/00: Pharmacokinetics of GW572016X following oral administration of GW572016Fand GW572016X at 10 mg/kg GW572016X to male beagle dogs

Male dogs were fasted and administered a single administration of GW572016 as the free base, GW572016X, or the ditosylate salt, GW572016F, in a cross-over design, and blood samples were collected for 48 hrs. As was seen in the rat, exposure levels are higher when the fasted dogs are administered the salt formulation of GW572016.

Pharmacokinetic Parameters of GW572016X in Fasted Male Beagle Dogs							
Compound		AUC_{∞} (h*ng/mL)	C_{max} (ng/mL)	T_{max} [1] (h)	$t_{½}$ (h)	Dose-Normalized [2] AUC	C_{max}
GW572016F	Mean	4934	543	1-4	2.86	4586	504
	SD	2204	208		1.09	2088	193
GW572016X	Mean	3094	291	2-4	4.17	3022	284
	SD	3652	316		2.83	3405	289

n = 4 or 6

1. The T_{max} described as a range rather than a mean.
2. AUC and C_{max} were dose-normalized to 10 mg/kg.

[Table excerpted from Sponsor]

2.6.4.4 Distribution

RD2000/00355/01: The *in vitro* binding of GW572016X to plasma proteins and erythrocyte partitioning in mouse, rat, rabbit, dog and human

The *in vitro* protein binding of GW572016 was determined in mouse, rat, rabbit, dog and human plasma and blood. Plasma samples were incubated with [^{14}C]-GW572016 and counted by liquid scintillation. Additional plasma samples were centrifuged and aliquots of filtrate were counted in a liquid scintillation counter. Plasma protein binding was determined and in all species exceeded 99% at nearly every concentration of GW572016 tested. Whole blood samples were spiked with [^{14}C]-GW572016 and incubated then counted for radioactivity. Additional blood samples were centrifuged to separate the plasma from the RBCs and the plasma samples counted for radioactivity. These data were used to determine the percent binding to erythrocytes. Erythrocyte binding was greater in the rabbit and dog, with plasma:blood ratios indicative of approximately equal distribution. In the mouse, rat and human blood there was no preferential uptake of GW572016 into the erythrocytes, showing that GW572016 selectivity for plasma in these species.

[^{14}C]-GW572016X Conc. (µM)	Ratio of whole Blood Concentration to Plasma Concentration (Study Number 00AVT0011)				
	Mouse (male)	Rat (male)	Rabbit (male)	Dog (male)	Human (male + female pool)
100	0.76 ± 0.11	0.54 ± 0.07	0.91 ± 0.08	0.92 ± 0.11	0.88 ± 0.11
25	0.66 ± 0.10	0.51 ± 0.02	0.87 ± 0.03	0.99*	0.63 ± 0.04
10	0.68 ± 0.08	0.46 ± 0.01	0.92 ± 0.05	1.02 ± 0.02	0.78 ± 0.06
5	0.60*	0.41 ± 0.08	1.13 ± 0.16	0.85 ± 0.14	0.84 ± 0.13
1	0.78 ± 0.03	0.47 ± 0.03	1.95 ± 0.34	0.95 ± 0.13	0.79 ± 0.06

n = 3 replicate determinations except the data point with * where n=2

[Table excerpted from Sponsor]

RD1999/02816/00: ^{14}C-GW572016: Quantitative wholebody autoradiography following oral administration (10 mg[base]/kg) to the albino and pigmented rat

A single oral dose of 10 mg/kg of [^{14}C]-GW572016 was given to Wistar Han albino rats and pigmented Lister Hooded rats. At time intervals ranging from 0.5 to 168 hrs after administration tissue distribution of the radioactive GW572016 material was measured using whole-body autoradiography and digital images obtained by phosphorimaging were quantified. The table below shows relevant tissues and levels of GW572016. It is clear

that there was not extensive absorption of the drug after oral administration. Radioactivity is primarily found in the GI mucosa, the GI contents and the bile ducts, with very little found in the blood. When radioactivity was found in other tissues, it was relatively evenly distributed, with the highest levels seen in the lung, spleen, kidney, liver, preputial gland, esophagus, pituitary, adrenal cortex and to a lesser extent the adrenal medulla. The uveal tract levels are higher in the pigmented rat than the albino rat. Other tissue distributions were comparable and therefore combined for the table. Little radioactivity was found in the CNS. Radioactivity was largely cleared from the system at 24 hrs.

Concentrations of Radioactivity in Varying Tissues Measured at 4 hrs After Administration of 10 mg/kg of ^{14}C-GW572016	
	Average Levels in all Rats (µg equiv/g)
Small intestine mucosa	12.03
Cecum mucosa	2.21
Stomach contents	56.87
Small intestine contents	101.8
Cecum contents	59.37
Large intestine contents	4.14
Bile ducts	27.62
Esophagus	4.57
Liver	5.55
Spleen	3.41
Lung	4.22
Kidney cortex	3.40
Adrenal cortex	5.62
Adrenal medulla	3.52
Pituitary	2.18
Preputial gland	3.10
Blood	0.92
Uveal tract	3.59 (Lister-Hooded) 0.45 (Wistar Han)

2.6.4.5 Metabolism

RD2000/01947/00: *In vitro* metabolism of GW572016 using 1) heterologously-expressed recombinant human CYP450 enzymes and 2) pooled human liver microsomes with a CYP3A4/5 selective inhibitor

Heterologously-expressed recombinant human CYP450 enzymes and pooled human liver microsomes with a CYP3A4/5 selective inhibitor were used to identify the CYP450 isozymes responsible for the metabolism of GW572016 *in vitro*. The CYP1A2, CYP2A6, CYP2B6, CYP2C8, CYP2C9, CYP2C19, CYP2D6, CYP2E1, CYP3A4, and CYP3A5 recombinant enzymes were incubated separately with ^{14}C-GW572016 and then

the incubations analyzed by HPLC with UV and radiochemical detection. Negative controls were samples with no NADP included. Pooled human liver microsomes were incubated with two GW572016 concentrations and with and without ketoconazole, the CYP3A4/5 inhibitor.

GW572016 metabolism was detected in CYP2C8, CYP3A4, and CYP3A5 expressed microsomes. Complete inhibition of GW572016 metabolism occurred in the presence of ketoconazole and 3.1 µg/mL of GW572016 and 89% inhibition with a lower concentration of 0.31 µg/mL. These results indicate that GW572016 is metabolized primarily by CYP3A4 and CYP3A5, with minor metabolism by CYP2C8. Results are presented below, showing the percentage of metabolism seen in each enzyme assay.

Recombinant Human CYP450 Enzymes	Total % Peak Areas of GW572016 Metabolites[1]
CYP1A2	-[2]
CYP2C9	-
CYP2C19	5%
CYP2D6	-
CYP3A4	69%
CYP3A5	30%
CYP2B6	-
CYP2A6	-
CYP2E1	-
CYP2C8	15%

1. The percentage of metabolism was calculated by summing the % peak areas of the metabolites (NADP-dependent peaks) of GW572016 formed in each incubation.
2. No NADP-dependent peaks were observed.

[Table excerpted from sponsor]

RD2005/00052/00: An *in vitro* investigation of the enzymes involved in the formation of alkylamine N-oxidation metabolites of 14C-GW572016 using human liver microsomes and heterologously-expressed human cytochrome P450 and flavin-containing monooxygenase enzymes

Previous studies have shown that CYP3A4, CYP3A5 and to a lesser extent CYP2C8 are involved in the major metabolic pathway of GW572016, O-dealkylation. The other

metabolic pathway of GW572016 is a cascade of metabolites produced by N-oxidation and/or α-carbon oxidation. This study was designed to determine the CYP450 isoforms that are responsible for this metabolic pathway. The table below shows the percentage of GW572016 metabolized via these pathways. Again, CYP3A4 and CYP3A5 are the primary isozymes involved in this metabolic pathway, with CYP1A2, 2C8, 2C9, 2C19, and 2D6 also involved. Ketoconazole incubated with human liver microsomes abolished > 99% of the N-oxidation and/or α-carbon oxidation metabolic peak areas.

	Total % Peak Area of N-oxidation and/or α-carbon Oxidation Metabolites	
Enzyme Matrix	3 µM [^{14}C]-GW572016	50 µM [^{14}C]-GW572016
Human Liver Microsomes	3.7%	4.2%
CYP1A2	2.6%	0.92%
CYP2A6	-[1]	-[1]
CYP2B6	-[1]	-[1]
CYP2C8	9.4%	0.68%
CYP2C9	4.7%	0.71%
CYP2C19	1.5%	0.20%
CYP2D6	5.4%	1.8%
CYP2E1	-[1]	-[1]
CYP3A4	10%	11%
CYP3A5	3.9%	7.2%

1. No NADPH dependent peaks were observed
((∑ % metabolite peak areas with cofactor) – (∑ % metabolite peak areas without cofactor))/ Total Peak Area) x 100

[Table excerpted from sponsor]

APPEARS THIS WAY
ON ORIGINAL

RD2002/01185/00: An *in vitro* evaluation of the inhibitory potential of GW572016 on human cytochrome P450 enzymes

Human pooled liver microsomes were used to analyze the inhibition of CYP3A4 and CYP3A5 by GW572016 by using testosterone 6β-hydroxylation and midazolam 1'-hydroxylation as markers for CYP3A4/5 activity. The markers were analyzed using HPLC and then computer software used to calculate IC_{50} and Ki values, which are shown in the table below. The results show that *in vitro*, GW572016 is a competitive and non-competitive inhibitor of CYP3A4/5. Determination of the IC_{50} using seven concentrations of GW572016 (0.5 – 50 μM) also showed that at ≤ 5 μM, GW572016 increased enzyme activity of CYP3A4/5.

Enzyme	CYP Activity	IC_{50} (μM)	Ki (μM)
CYP3A4/5	testosterone 6β-hydroxylase	7.1 ± 0.8	4.0 ± 1.0*
CYP3A4/5	midazolam 1'-hydroxylase	39 ± 14	ND**

* - mixture of competitive/non-competitive inhibition
** - non Michaelis-Menten kinetics

RD2001/01300/00: An *in vitro* evaluation of the inhibitory potential of GW572016 on testosterone 6b-hydroxylase and midazolam 1-hydroxylase activity in human liver microsomes

Human liver microsomes were incubated in the absence or presence of varying concentrations of GW572016 and probe substrates for CYP1A2, CYP2C9, CYP2C19, and CYP2D6. Enzyme activity was measured by specific assays for each isozyme, phenacetin O-deethylation (CYP1A2), diclofenac 4'-hydroxylation (CYP2C9), S-mephenytoin 4'-hydroxylation (CYP2C19) and bufuralol 1'-hydroxylation (CYP2D6) and IC_{50} values calculated. The results are presented below and show GW572016 inhibited CYP2C9 and CYP2D6, moderately inhibited CYP2C19 and weakly inhibited CYP1A2.

Cytochrome P450 Enzyme	**Activity Measured**	**IC_{50} (μM)**
CYP1A2	Phenacetin O-deethylation	>30
CYP2C9	Diclofenac 4'-hydroxylation	11.8
CYP2C19	S-Mephenytoin 4'-hydroxylation	27.2
CYP2D6	Bufuralol 1'-hydroxylation	13.8

RD2004/00416/00: An *in vitro* evaluation of GW572016 as an inducer of cytochrome P450 expression in cultured human hepatocytes

Human hepatocytes were cultured and varying concentrations of GW572016 or prototypical inducers of CYP1A2 (3-methylcholanthrene), CYP2C9 and CYP3A4 (rifampicin) were added daily for 3 days. Enzyme activity was measured by using the

rate of formation of markers specific for each enzyme and mRNA expression was analyzed by TaqMan assay. The tables below show that GW572016 did not increase the enzymatic activity in any of the three isoforms, nor did it increase the mRNA levels in CYP1A2 or CYP2C9 and only weakly increased CYP3A4 mRNA. This indicates that there is little potential for GW572016 to induce these CYP450 enzymes.

Enzymatic Activity (pmol/mg protein/min)			
Treatment	7-Ethoxyresorufin O-dealkylation [1] (CYP1A2)	Diclofenac 4'-hydroxylation [2] (CYP2C9)	Testosterone 6β-hydroxylation [2] (CYP3A4)
Control, 0.1% DMSO	4.2 (1.0) [3]	1281 (1.0)	1743 (1.0)
3 µM GW572016	10 (2.3)	737 (0.6)	2198 (1.3)
10 µM GW572016	12 (3.0)	1579 (1.2)	3281 (1.9)
30 µM GW572016	6.4 (1.5)	958 (0.7)	1304 (0.7)
50 µM GW572016	7.5 (1.8)	1419 (1.1)	1376 (0.8)
10 µM 3-MC [4]	41 (10)	ND [5]	ND
20 µM Rifampicin	ND	2689 (2.1)	5732 (3.3)

1. Values are the mean of 3 human hepatocyte preparations (Hu122, Hu126, Hu141)
2. Values are the mean of 4 human hepatocyte preparations (Hu121, Hu122, Hu126, Hu141)
3. Values in parentheses represent fold change relative to control
4. 3-methylcholanthrene
5. ND: Not determined

[Table excerpted from sponsor]

mRNA Expression (mRNA copies/ng Total RNA)			
Treatment	CYP1A2[1]	CYP2C9[2]	CYP3A4[2]
Control, 0.1% DMSO	233 (1.0) [3]	2268 (1.0)	996 (1.0)
3 µM GW572016	303 (1.3)	1656 (0.73)	1597 (1.6)
10 µM GW572016	300 (1.3)	2527 (1.1)	2501 (2.5)
30 µM GW572016	184 (0.79)	1242 (0.55)	3153 (3.2)
50 µM GW572016	202 (0.87	2532 (1.1)	2939 (3.0)
10 µM 3-MC[4]	6703 (29)	ND [5]	ND
20 µM Rifampicin	ND	6667 (2.9)	15348 (15)

1. Values are the mean of 3 human hepatocyte preparations (Hu122, Hu126, Hu141)
2. Values are the mean of 4 human hepatocyte preparations (Hu121, Hu122, Hu126, Hu141)
3. Values in parentheses represent fold change relative to control
4. 3-methylcholanthrene
5. ND: Not determined

[Table excerpted from sponsor]

RD2004/02884/00: Quantitative Metabolite Profiling and Metabolite Identification in Plasma, Bile and Feces of CD-1 Mice Administered [^{14}C]-GW572016 Orally as a Suspension at 30 mg free base/kg

The plasma, bile, urine and feces collected from mice used in an excretion-balance study were analyzed for profiles of [^{14}C]-GW572016-related material using HPLC with radiochemical detection. The major route of elimination in the mouse is by metabolism of GW572016, with the metabolites, for the most part, excreted in the bile. Most of the GW572016 found in the plasma was found as the parent compound, with the metabolites including U19233-1-2 (O-dealkylation, sulfation) and M1 (oxidation, glucuronidation) and N-dealkylation, conjugation and N-oxidation products.

RD2003/00475/01: Profiling and identification for metabolites of GW572016 in the Sprague-Dawley rat following a single oral administration of 14C-GW572016 at 10 mg free base/kg

Plasma and feces from intact and bile duct-cannulated rats were analyzed to quantify and structurally identify the major metabolites of GW572016 after administration of 10 mg/kg of [^{14}C]-GW572016. HPLC with radiochemical detection was used to determine metabolic profiles while NMR and mass spectrometry was conducted to identify the structural characterizations of the isolated metabolites. Metabolites included the principal route of metabolism, O-dealkylation to GW690006, which was further metabolized to an O-glucuronide conjugate (U19233-1-1) and a sulfate conjugate (U19233-1-2). Other metabolites are formed by N-dealkylation of GW572016 to the amine GW819480, a carboxylic acid (GSK342393) and a furan rearrangement of GW572016 to generate GW815070. The table below lists these and other metabolites found in feces and bile.

Peak ID	% Dose Mean				
	Feces (Intact Male)	Feces (Intact Female)	Feces (BDC Male)	Bile (BDC Male)	Total (BDC Bile + Feces)
GW572016 * GW815070	11.8	22.9	26.7	2.5	29.2
M4	7.6	3.8	0.8	ND	0.8
U19233-1-1	ND	ND	ND	6.8	6.8
GW690006	50.0	34.0	4.6	1.0	5.6
U19233-1-2	ND	ND	ND	31.6	31.6
M2	3.7	3.6	0.2	ND	0.2
GSK342393	3.4	5.5	0.2	2.0	2.2
Total	76.4	69.7	32.4	43.8	76.3

n = 3 intact males, 3 females and 3 BDC males.

* GW572016 and GW815070 co-eluted in feces, but GW815070 was not detected in bile.

ND = Not Detected.

[Table excerpted from sponsor]

RD2004/01115/00: Metabolite Profiling Identification in Plasma and Feces of Rats Administered [14C]-GW572016 Orally as a Suspension at 10 mg free base/kg

This study was a further examination of the metabolites in rat feces, bile and plasma. In study RD20003/00475/01 it was noted that a poorly resolved shoulder, identified as GW815070, eluted with [^{14}C]-GW572016 in fecal stability and post-dose homogenates which had originally been prepared in water. This study had two fecal homogenate stability samples, one prepared in water and one prepared in 50% (v/v) ethanol/water. Liquid scintillation counting was used to monitor recovery of radiocarbon and radio-HPLC to characterize the metabolites. Results from this study indicate that GW815070, recovered in a previous study, arose from decomposition of GW572016 during processing. The major metabolites of GW572016, primarily found in the feces, arose from O- or N-dealkylation, sulfation and furan ring arrangement. The mean recovery of radiocarbon in the feces was 80.9% and the table below shows the main metabolites found in the rat feces.

Peak ID	RT (min)	Mean % of Dose
GW572016	33.8	18.8
GW690006	5.3	42.3
U19233-1-2	13.5	6.5
M2	46.0	2.8
GSK342393	56.2	1.9
Total		72.4

Mean of 3 rats.

[Table excerpted from sponsor]

Feces from dogs used to examine the excretion and elimination of GW572016 was further analyzed using HPLC UV and radiochemical detection to determine the metabolic profile of ^{14}C- GW572016-related material.

RD2002/00072/00: Identification of the metabolites of GW572016 in the dog

Samples of plasma and feces from dogs administered single oral doses of 10 mg/kg [^{14}C]-GW572016 were analyzed by a combination of radio-LC, LC/MS, and tandem mass spectrometry (MS/MS) to identify the major metabolites in the dog. The major components found in the feces were identified as GW572016 and GW690006 and only GW572016 was detected in plasma.

RD2004/00932/00: Profiling and identification for metabolites of GW572016 in humans after single oral administration of 14C-GW572016

Human plasma and excreta were collected from a healthy volunteer study where subjects were given a single oral suspension of 250 mg [^{14}C]-GW572016. Radiochemical profiling of [^{14}C]-GW572016-derived radiocarbon was determined by HPLC combined with radiochemical flow detection. Structural characterization was done by conducting synthetic oxidation reactions with GW572016 to magnify the production of putative metabolites to allow for greater quantities of metabolite to be analyzed by mass spectrometry and NMR and to then be used as for comparison with the blood and feces metabolite determination, also done by MS and NMR.

Unchanged GW572016 accounted for 30% of the administrated drug found in the feces, indicating the elimination of GW572016 was primarily via metabolism. Identified in the feces were GW690006 (an O-dealkylation product of the parent compound), M3 (a mono-oxidation product GW690006), GW815070 (a rearrangement of GW572016 to a pyridium salt), M^2 (a hydroxypyridine possibly from the loss of a methylethylsulfone from GW815070) and GSK342393 (a carboxylic acid). In plasma, GW572016 accounted for approximately half of the radiocarbon recovered and the remaining radiocarbon was accounted for by metabolites that were detected by LC/MS but below the limits of radiochemical detection. These components included a hydroxylamine (GSK203042), 2-oximes, 2-nitrones, an aldehyde (GW560231, further characterized in several local tolerance studies), and a carboxylic acid (GSK342383) metabolite of GW572016.

The figure below shows a proposed pathway for the metabolism of [^{14}C]-GW572016 in healthy human subjects.

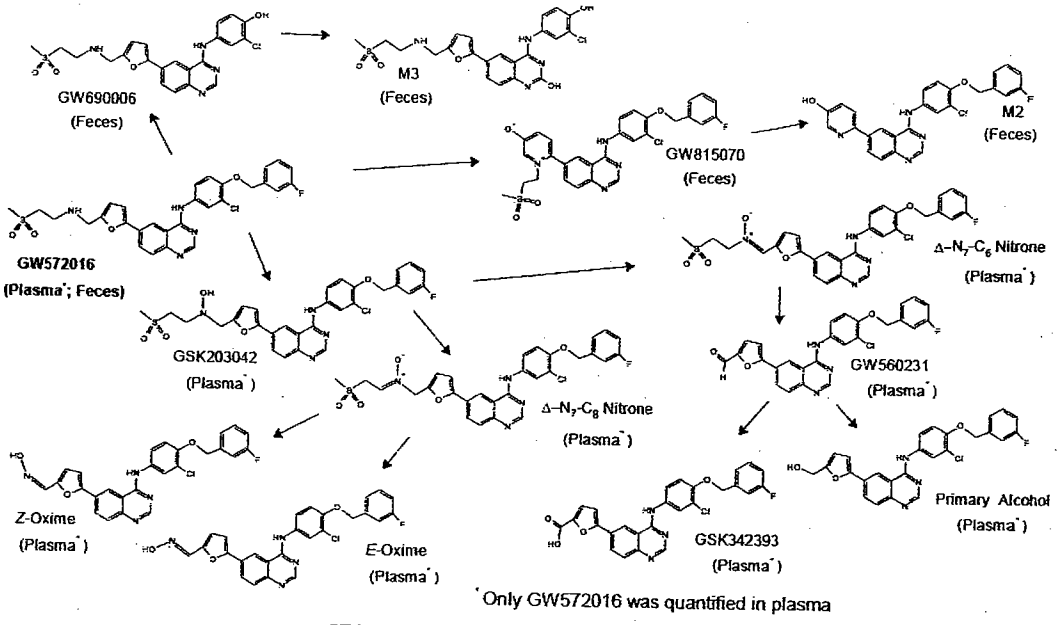

[Figure excerpted from sponsor]

RD2003/00727/02: GW572016: Radioanalysis of samples following single 250 mg oral suspension dose of [14C]-GW572016 to healthy volunteers 7274-208

The rate and extent of metabolism of [^{14}C]-GW572016 after administration of 250 mg orally to healthy subjects was examined in 6 individuals (3/gender). Urine and plasma were obtained at intervals beginning at 15 min post-dose and up to 168 hr after administration. Samples were analyzed by liquid scintillating counting for levels of $^{14}CO_2$ formed from sample combustions conducted with a — -Sample Oxidizer. Samples from this study were then used in study RD2004/00932/00 for the characterization of the metabolites of GW572016 found in the plasma and the feces. The figure below shows that the predominant route of elimination was the feces (median of 91.8%) with a median of 1.16% found in the urine.

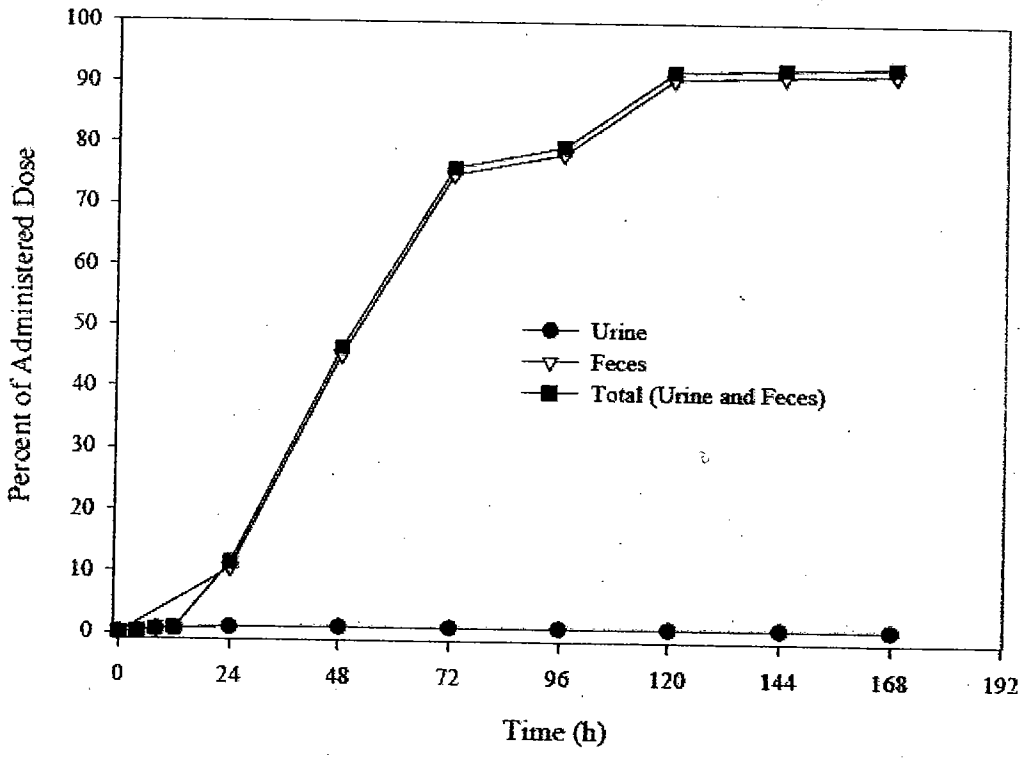

[Figure excerpted from sponsor]

The figure below shows the median plasma concentrations of radioactivity in subjects after the single oral dose of [^{14}C]-GW572016. The highest median concentration is seen at 4 hrs and with a level of 712 ng equiv/g.

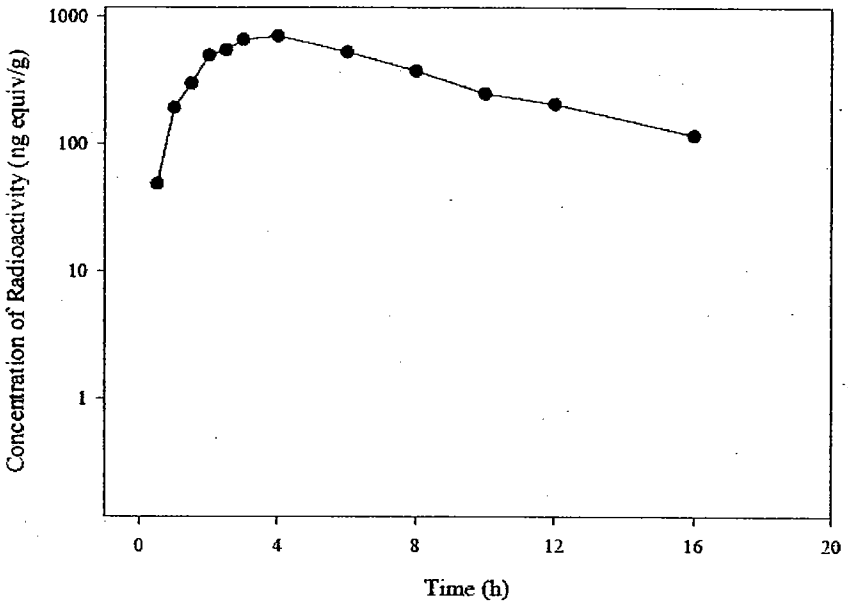

[Figure excerpted from sponsor]

2.6.4.6 Excretion

RD2004/01116/00: Elimination of radioactivity following a single oral administration of ^{14}C-GW572016 to male and female intact and male bile duct cannulated mice

RD2002/01538/00: Elimination of radioactivity following a single oral (10 mg/kg) administration of ^{14}C-GW572016 to male and female intact and male bile duct-cannulated rats

Two studies examined the elimination of radioactivity after a radiolabeled GW572016 was orally administered to intact and bile duct cannulated mice and rats. Sample combustions were performed with a — ample Oxidizers and $^{14}CO_2$ was trapped then radioactivity content quantitated by liquid scintillation counting. In the mice, approximately 90% of the radioactivity was recovered in urine and feces (88.7% in males and 91.2% in females). The elimination was primarily through the feces with 85.8% and 88.5% of the radiocarbon found in the males and females, respectively.

Blood, plasma and liver exposures to [^{14}C]-GW572016 were also examined in the intact mice. Results showed that the radiocarbon partitioned slightly more into plasma than the cellular fraction of blood and that liver exposure was 12- to 20-fold higher in the liver than the blood. The first two figures clearly show the fecal elimination of GW572016 in male and female intact mice. The figure that follows shows that concentration of GW572016 in the liver versus blood over time.

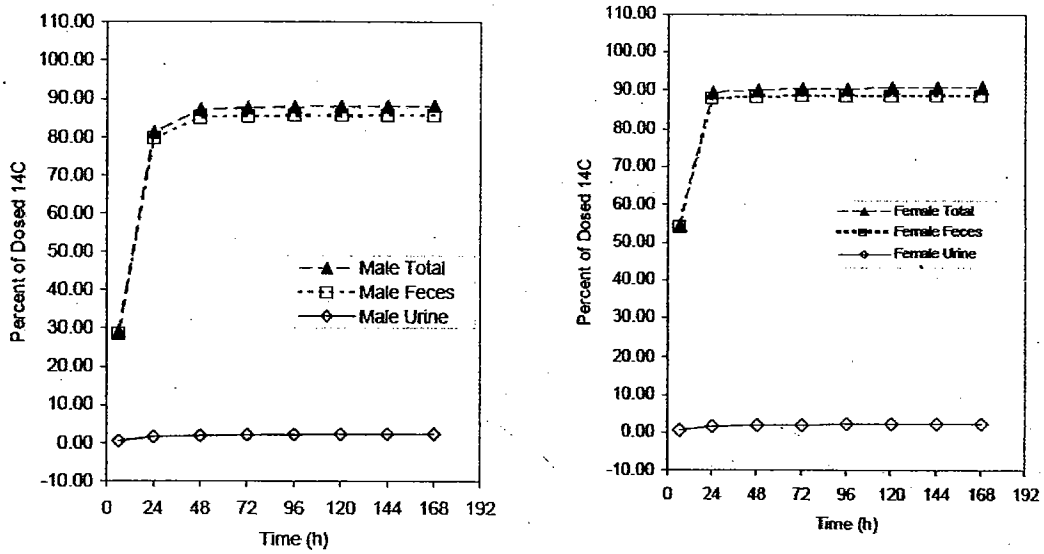

[Figures excerpted from sponsor]

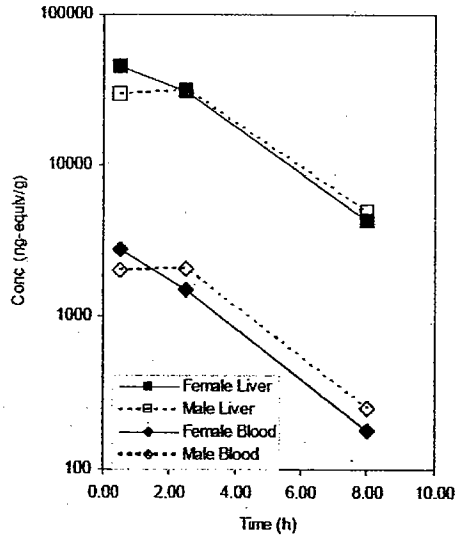

[Figure excerpted from sponsor]

When bile duct-cannulated mice received a single oral dose of radiolabeled GW572016, 91.5% of the radiocarbon was recovered, with 3.4% in the urine, 41.9% in the bile and 40.3% in the feces. The combined recovery of radiocarbon in the urine and bile indicates that 44% of the 30 mg/kg dose of GW572016 was absorbed.

Paclitaxel is one such agent and is a compound primarily metabolized by CYP2C8 and to a lesser extent by CYP3A4. Pooled human liver microsomes were used to assess the GW572016 effect on the rate of formation of two paclitaxel metabolites. The graphs below show IC_{50} values for GW572016 inhibition on the rate of formation of the two metabolites, Figure A is for the metabolite formed by CYP3A4 and Figure B for the metabolite formed by CYP2C8. The IC_{50} values show that GW572016 significantly inhibits the formation of both metabolites.

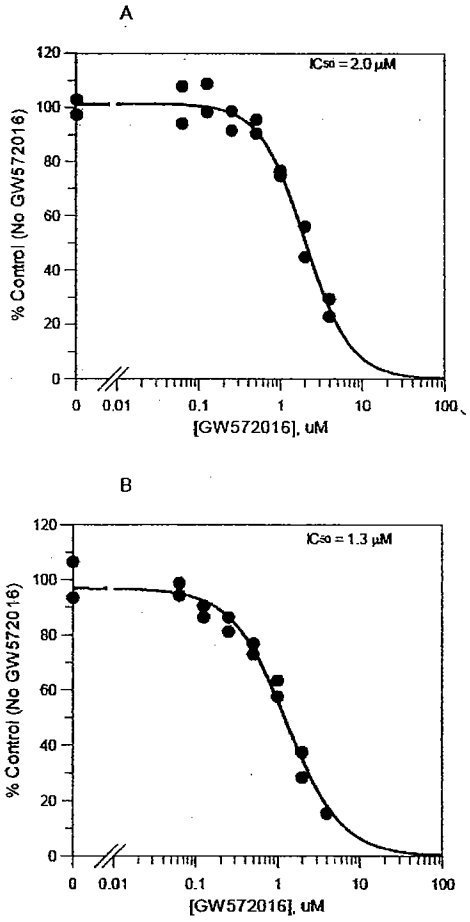

[Figure excerpted from sponsor]

To determine the type of inhibition, the Ki was obtained and then fit into a Michaelis-Menten competitive inhibitory model. The resulting Ki values, relative to the IC_{50} values, were indicative of competitive inhibition, where IC_{50}=2Ki. These values are shown in the table below, along with positive controls for each P-450 enzyme and the kinase inhibitor gefitinib.

Inhibitor	CYP3A4		CYP2C8	
	IC_{50} (μM)	K_i (μM)	IC_{50} (μM)	K_i (μM)
GW572016F	2.0	1.1	1.3	0.60
Iressa®	12	7.2	12	6.5
Ketoconazole	0.030	ND	ND[1]	ND
Quercetin	ND[1]	ND	2.5	ND

ND = Not Determined

[Table excerpted from sponsor]

RD2001/01665/00: The inhibition of paclitaxel, docetaxel, and vinorelbine metabolism by GW572016X in pooled human liver microsomes

Another *in vitro* study obtained similar results for the inhibition of paclitaxel by GW572016. To measure the ability of GW572016 to inhibit docetaxel and vinorelbine the disappearance of parent compound was used as the marker for CYP3A4 mediated metabolism with these two drugs. Inconclusive results were seen with the metabolism of docetaxel and the results with vinorelbine, though a modest increase in the half-life of the drug was seen with the highest concentration of GW572016.

RD2002/00921/00: The *in vitro* inhibition of GW572016X metabolism by paclitaxel, docetaxel and vinorelbine in pooled human liver microsomes

A third study examined the converse effect, the ability of paclitaxel, docetaxel and vinorelbine to inhibit the metabolism of GW572016 in pooled human liver microsomes. The rate of formation of the GW572016 metabolite GW690006, formed primarily by CPY3A4/5 metabolism, was determined. Then the rate of this formation was measured using GW572016 incubated with varying concentrations of the three drugs and the IC_{50} calculated. The figure and table below show that docetaxel inhibited the metabolism of GW572016 more than the other two compounds and did so at a C_{max} that was comparable to the levels seen clinically. Complete inhibition was not seen with paclitaxel so the IC_{50} was estimated.

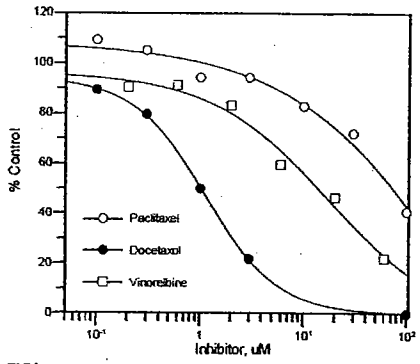

[Figure excerpted from sponsor]

Drug	IC_{50} µM
docetaxel	1.3
vinorelbine	13.2
paclitaxel	(30-70)*

* estimated by visual inspection of inhibition curves

[Table by reviewer]

2.6.4.8 Other Pharmacokinetic Studies
None conducted

2.6.4.9 Discussion and Conclusions

Oral bioavailability of lapatinib is 50.0%, 24.0 -28.7% and 41.9 - 63.2% in mouse, rat and dog, respectively following a 10 mg/kg dose, as determined in several studies. In most of the toxicology studies a dose-proportional increase in drug exposure was seen with increasing doses of lapatinib with little indication of drug accumulation over time. The drug is nearly completely plasma protein bound. There is limited absorption of lapatinib when taken orally in the rat when whole-body autoradiography was conducted, as the majority of the drug component was found in the GI tract and the bile ducts. The tissues where small but significant amounts of the drug were found included the liver, pituitary, lung, adrenal gland, preputial gland and kidney. There was not extensive CNS distribution. The drug does bind to melanin, as evidenced by the binding to the uveal tract in pigmented animals. Despite that, no toxicology studies have shown any histological ophthalmic abnormalities. Lapatinib is primarily metabolized by O-dealkylation to the phenol GW690006 and is predominantly CYP3A4/5 mediated. Excretion is primarily through biliary excretion into the GI tract and >82-99% of the drug was accounted for in the feces in the mouse, rat and dog. Additionally, in humans the majority of the drug is eliminated in the feces. The metabolism of lapatinib is similar across species with no unique human metabolites identified. *In vitro* assays with human hepatocytes show that lapatinib has minimal potential to induce CYP3A4/5 and has potential to inhibit CYP3A4, 1A2 and 2C8.

The human AUC presented in the comparative summary is 36.2 µg/mL, however a value of 46 was obtained in a study where lapatinib and capecitabine were combined. As the regimen being proposed for this application is for the combination, where applicable the AUC from the combination study was used if a human AUC was needed.

2.6.4.10 Tables and figures to include comparative TK summary

Species (Duration)	Dose (mg/kg)	Sex	C_{max} (ng/mL) [range]		AUC_{tau-tf} (ng.h/mL) [range]		Ratio of Animal to Human Exposure	
			Day 1	End of Study	Day 1	End of Study	C_{max}	AUC
Rat (14 day)	1000	M	7507 [3277-14161]	37447 [22130-46110]	297944	773341	15.4	21.4
		F	37015 [10123-54531]	114805[1]	1131015	946503[1]	47.2	26.1
Rat (6 month)	20	M	1411 [1227-1712]	2435 [1788-2758]	5117	10455	1.0	0.29
	10[3] (NOAEL)	**F**	**1916 [812-2572]**	**3710 [2324-4563]**	**12745**	**25052**	**1.5**	**0.69**
	60[3] (NOAEL)	**M**	**3998 [3493-4453]**	**3854 [3035-5080]**	**20424**	**24705**	**1.6**	**0.68**
		F	12616 [9739-15114]	22733 [12755-28977]	134044	207267	9.4	5.7
	180	M	8213 [4301-12125]	7236 [3902-9537]	68118	71680	3.0	2.0
	120	F	38329 [38329-38818]	27631 [21806-34831]	369941	414998	11.4	11.5
Human (14 Day)	32[2]	M		2430[2]		36200[2]	NA	NA

Key:
NA = Not applicable.
1. Final toxicokinetic assessment on Day 10 for females given 1000 mg/kg/day. Data presented are from one animal.
2. Human exposure at 1250 mg/day, 25 mg/kg/day in a 50 kg human at steady state (Clinical Study EGF10005).
3. No observed adverse effect level (NOAEL). Note in the rat study the NOAEL differed between males and females; exposure ratios in bold text are at the NOAEL.

Species (Duration)	Dose (mg/kg)	Sex	C_{max} (ng/mL) [range]		AUC_{tau-tf} (h.ng/mL) [range]		Ratio of Animal to Human Exposure	
			Day 1	End of Study	Day 1	End of Study	C_{max}	AUC
Dog (9 month)	**10[1] (NOAEL)**	**M**	**545 [326-753]**	**652 [197-1360]**	**4278 [2008-6704]**	**5425 [1159-12516]**	0.27	0.15
		F	**598 [401-828]**	**1018 [677-1485]**	**4422 [2298-7131]**	**8155 [7151-11621]**	0.42	0.23
	40	M	2843 [1643-4094]	1467 [1018-1830]	36112 [20391-48769]	18700 [8161-28415]	0.60	0.52
		F	2197 [1500-2599]	3521 [2819-4423]	28468 [10951-40884]	54450 [30202-65625]	1.4	1.5
	100	M	6105 [3833-8429]	4466 [3750-5643]	94448 [47759-147729]	70797 [57068-82472]	1.8	2.0
		F	6784 [4086-8054]	4734 [1803-7833]	101156 [65127-138545]	77239 [34710-116780]	1.9	2.1
Human (14 Day)	32[2]	M		2430[2]		36200[2]	NA	NA

Key:
NA = Not applicable.
1. No observed adverse effect level (NOAEL). Exposure ratios in bold text are at the NOAEL.
2. Human exposure at 1250 mg/day, 25 mg/kg/day in a 50 kg human at steady state (Clinical Study EGF10005)..

2.6.5 PHARMACOKINETICS TABULATED SUMMARY

See 2.6.4.10

2.6.6 TOXICOLOGY

2.6.6.1 Overall toxicology summary

General toxicology:
The general toxicology of lapatinib has been examined in several laboratory animals: mouse, rat, and dog using the IV and PO routes of administration. Single dose studies were conducted in the mouse and rat using the IV and PO routes. The primary toxicities were not identified in these studies, nor were lethal doses of lapatinib reached.

Repeat-dose toxicity was examined in the mouse, rat, and dog using the PO route. The pivotal rat study was a six-month PO study (120, 360 and 1080 mg/m^2 in males and 60, 360 and 720 mg/m^2 in females). In this study the effects seen with lapatinib administration included reddening of the skin, scabbing and flaking of the tail. Most of the toxicological findings were more prominent in the female rats. Increases in white blood cell parameters were seen at HD males and MD and HD females. Lapatinib was also associated with increases in ALT, cholesterol and bile acids. Female HD rats had increased adrenal, kidney and liver weights, which correlates with increases in ALT. histopathological effects include pigmentation in several organs, mucosal hyperplasia and inflammation in the GI tract and hyperplasia in the lymph nodes. Histopathological evidence of skin toxicity was also noted. Many of these effects are not surprising, considering the pharmacology of lapatinib. In particular, the skin effects are most likely a direct EGFR inhibitory effect. The chronic rat study, among others, also showed evidence of liver toxicity following long-term treatment with lapatinib. The principal route of excretion of lapatinib is hepatobiliary, as mass balance studies have shown the majority of the drug is found in the feces. Other rat studies have shown degeneration/necrosis of skeletal muscle including the eye muscles and the tongue. Additional histopathology includes erosion of the stomach epithelium, prostate atrophy, adrenal hypertrophy, alveolar histocytosis in the lungs, lymphoid depletion, trabecular atrophy of the femur joint and zymogen granule depletion in the pancreas.

A toxicology study for 28-days with the genotoxic impurity — (90, 900, 3000 mg/m^2) was also conducted. Most of the toxicities were similar to the toxicities seen with lapatinib. The impurity did lead to increased bilirubin and methemaglobin and disruption of the urinary bladder epithelium.

The pivotal dog repeat-dose study was conducted for 39 weeks with lapatinib in gelatin capsules (200, 800 and 2000 mg/m^2/day). Liver toxicity was evident in this study, with high levels of ALT, ALP, bile acids and bilirubin. Bilirubin was found in large levels in the urine of some of the HD dogs as well and ophthalmologic exams indicated evidence of jaundice. Concurrent histopathological changes in the liver were also seen, including, inflammation, degeneration and cholestasis. Not surprising, skin toxicity was evident as paw lesions and skin redness were noted along with histopathological changes in the skin. GI, lymphoid tissue and adrenal gland effects were seen grossly and histopathologically.

Another common finding with drugs that act at the same target as lapatinib is adrenal gland toxicity, also seen in the dog study. The most prevalent histological finding was pigment deposition in numerous organs and tissues. This pigmentation was often the most common finding in a given tissue and not usually consistent with overt toxicity of that organ.

Genetic toxicology:
Lapatinib was tested for mutagenicity and clastogenicity in the *in vitro* Ames test, mouse lymphoma assay, human peripheral blood lymphocytes and the Chinese Hamster Ovary assay and in the *in vivo* rat bone marrow assay. In the doses tested in these studies, with and without metabolic activation, lapatinb was not mutagenic or clastogenic, with the exception of the results from the mouse lymphoma assay. In this study, lapatinib yielded an equivocal response at the 3-hr time point without S9 activation. An increased mutant frequency was seen in the lowest of seven concentrations tested in one of the 3-hr assays and at the third lowest concentration of the seven in the other study. The 24-hr assay was negative for mutagenicity. The tests with S9 could not be conducted as the drug precipitated and an appropriate level of toxicity could not be achieved. The *in vivo* rat bone marrow assay was negative for chromosomal aberrations at single oral doses of lapatinib up to 2000mg/kg.

Of interest when examining the genotoxic potential of lapatinib is the impurity [redacted] that is still present in the final product. During drug development, non-clinical studies with lapatinib used batches of the drug product with higher levels of [redacted] than is currently seen in the final clinical formulation. However, the current level of [redacted] still exceeds recommended limits. Current guidelines generally recommend that genotoxic impurity exposure not exceed 1.5 µg/day/person. The current specification limit for [redacted] is [redacted] which with the proposed daily dose of Tykerb (1250 mg/day) would result in a daily dose of [redacted].

The Ames test with [redacted] showed a dose-related reproducible statistically significant increase in revertant colony frequency when tested with metabolic activation. Another *in vitro* study, the mouse lymphoma assay, was also positive for mutagenicity. Two *in vivo* studies were conducted, the mouse micronucleus test and the rat bone marrow micronucleus test. In the mouse, single oral doses of 200 and 400 mg/kg [redacted] were mutagenic, and the lowest dose of 100 mg/kg was not. In the rat study, doses of 100 – 2000 mg/kg given on two consecutive days induced micronuclei. No micronuclei induction was seen $\leq$ 20 mg/kg.

Carcinogenicity:
Two-year carcinogenicity studies with lapatinib are currently ongoing in both the mouse and rat.

Reproductive toxicology:
Fertility studies in the rat were conducted with lapatinib with treated (120, 360 and 1080 mg/kg) males bred to untreated female and treated females bred to untreated males. No

effects were seen on male fertility when the male rats were treated prior to and throughout breeding. Mating and fertility indexes were comparable to controls and no adverse effects were seen on the outcome of the pregnancies (e.g., live birth index, number of implantations and corpora lutea, fetal body weights). The females bred with the MD males did have significantly lower gravid uterine weights and higher percent of pre- and post-implantation loss, though these were not statistically significant. There was a very minimal decrease in the number of live fetuses, though this wouldn't seem to account for the decrease in gravid uterus weights. This effect was not seen in the dams bred to the HD males, making the relationship with lapatinib tenuous. Of the 25 dams in the MD group, there were three with very small litters and large percentages of pre-implantation loss, including one rat with a litter of one and over 90% implantation loss. These few rats may be skewing the numbers.

When the female rats were dosed with lapatinib (120, 360 and 720 mg/m^2) during breeding and through the first six days of gestation, no changes in mating or fertility indexes were seen. There were, however, effects of this treatment on embryo-fetal development. Both the MD and HD litters had significantly lower fetal body weights compared to control. Gravid uterus weights were lower in both these groups as well. The HD dams had significantly increased percentage of implants that were resorbed and decreased numbers of live fetuses per litter.

The embryo-fetal development effects of lapatinib were studied in the rat and rabbit. In the rat, range-finding studies showed 1080 mg/m^2 to be clearly too maternally toxic to allow for an effective study with pregnant rats, as all these rats were euthanized moribund prior to the end of the study. A second range-finding study with 540 and 720 mg/m^2 showed the HD to lead to some maternal toxicity (body weight gains from GD 1 – 21 decreased by 35% compared to control and decreased by 50% from GD 7-20, the dosing period). This dose did not interfere with a successful pregnancy and was chosen as the HD for the pivotal embryo-fetal development study.

The pivotal rat study (180, 360 and 720 mg/m^2) did not show any teratogenic effects of lapatinib. There were a few variations seen, persistence of the left umbilical artery, presence of the 7th cervical rib and precocious ossification. No treatment-related malformations were seen. Maternal toxicity was seen, though it was minimal and included decreased food consumption during the period of dosing and decreased body weight gain from GD 7 – 18.

The pivotal rabbit study (360, 720, and 1440 mg/m^2) had increased abortions in the HD. The HD and MD rabbits had decreased body weights than the controls but when corrected for the gravid uterus, this difference was not significant. The decreased body weights are due more to the lower fetal body weights seen in these groups. In the HD rabbits that carried to term, the number of fetuses were not affected by the drug treatment so the gravid uterine effect can only be due to fetal weights. As to maternal toxicity, it was evident in the significantly decreased food intake seen in the HD does through the dosing period. Food consumption is generally considered the better indicator of maternal toxicity in rabbits. No drug-related incidence of malformations were seen in the

offspring, though a significant increase in alterations was seen in MD and HD offspring, due to soft tissue and skeletal variations.

The pre- and post-natal development of the rat was evaluated for the effects of lapatinib treatment (120, 360 and 720 mg/m^2). No effects of maternal doses up to the MD were seen on the pup development (e.g., learning/memory, locomotion, reproduction). The key finding in this study is the decreased neonatal viability in the HD rats. By PND 4, 91% of these pups were dead, while only 13% on the control pups were dead. A lung floatation test showed that these pups were born alive, yet there was no milk in their stomachs, so they did not nurse. Possible explanations for pups not nursing include lack of milk production, a possibility due to the effect of erbB-2 on mammary gland development, or dams that are either too sick to nurse their pups or who have behavioral alterations that would cause them to reject their litters. To determine if the problem was a maternal problem a cross-fostering study was conducted using a dose of 720 mg/m^2. Litters that were born to lapatinib-treated dams, but immediately fostered to control-treated dams, had 84 % of the pups dead by PND 8. Conversely, litters born to control-treated dams that were immediately fostered to lapatinib-treated females only 13% of the pups that were dead in the first week. This shows that the neonatal lethality is an effect of lapatinib on the pups and not on the dams or the milk production.

Special toxicology:
Special toxicology studies include local tolerance studies and an immunotoxicity study. Local tolerance studies were conducted using lapatinib as well as the lapatinib impurities — that structurally could be corrosive and the genotoxic — impurity —. Dermal and ocular irritation studies in the rabbit showed the main drug product, lapatinib, to pose negligible risk to the eye and characterized as a mild irritant to the skin. The skin result was due to one rabbit only that exhibited a slight erythema and edema that resolved within 72 hrs. The Draize classification was 0.3 with a 0 being a non-irritant. In the guinea pig skin sensitization test, lapatinib was not a skin sensitizer. An *in vitro* test showed — has little potential for ocular irritancy. — was a non-sensitizer, is not likely to cause dermal irritation and was a minimal irritant in the *in vivo* eye test.

The effect of a 28-day dosing regimen with three doses of lapatinib in the rat showed no effect of the treatment on the antibody response to the T-cell dependent antigen keyhole limpet hemocyanin (KLH).

2.6.6.2 Single-dose toxicity

Four single dose toxicity studies were conducted with lapatinib in the mouse and the rat, using the IV and oral routes of administration. These studies are briefly summarized below.

RD2000/00398/00: GW572016F: Single-dose intravenous toxicity study in CD-1® mice

This was a GLP study with two phases. In the first phase 6 mice (3/sex) were administered an IV dose of GW572016F, which is the monohydrate form of the ditosylate salt of the active test compound, GW572016X to determine the maximum nonlethal dose (MNLD). The targeted dose was 62.5 mg/kg but due to solubility problems the mice received an actual dose of 27 mg/kg. No deaths were seen in this phase. Adjustments were made to increase solubility and in the second phase of the study 6 mice/sex were administered a single IV dose that reached 73.4% of the target dose, or 46 mg/kg of GW572016. Mice were dosed on Day 1. Three mice/sex of both control and drug groups were euthanized on Day 3, 3/sex were euthanized on Day 15. No lethality was seen in the study. No effect of drug treatment was seen on body weights, which are shown in the figure below.

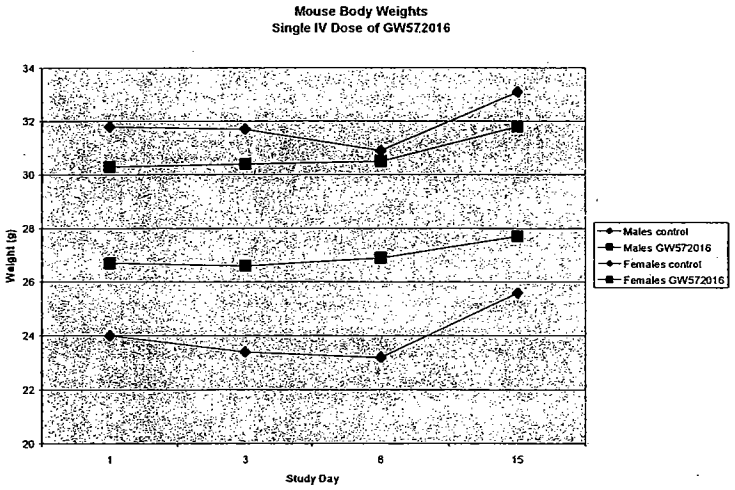

No significant effects of GW572016 IV administration were seen on macro- or microscopic observations.

RD2000/00192/00: GW572016F: Single-dose oral toxicity study in CD-1® mice

This was a GLP study with two phases. In the first phase 6 mice (3/sex) were administered an oral dose of 2000 mg/kg GW572016F, which is the monohydrate form of the ditosylate salt of the active test compound, GW572016X, to determine the maximum nonlethal dose (MNLD). As no mice died at this dose, it was used for the second phase. In the second phase of the study 6 mice/sex were administered a single oral dose of 2000 mg/kg of GW572016. Mice were dosed orally on Day 1. Three mice/sex of both control and drug groups were euthanized on Day 3, 3/sex were euthanized on Day 15. No

lethality was seen in the study. No significant effect was seen on body weights, as noted in the figure below.

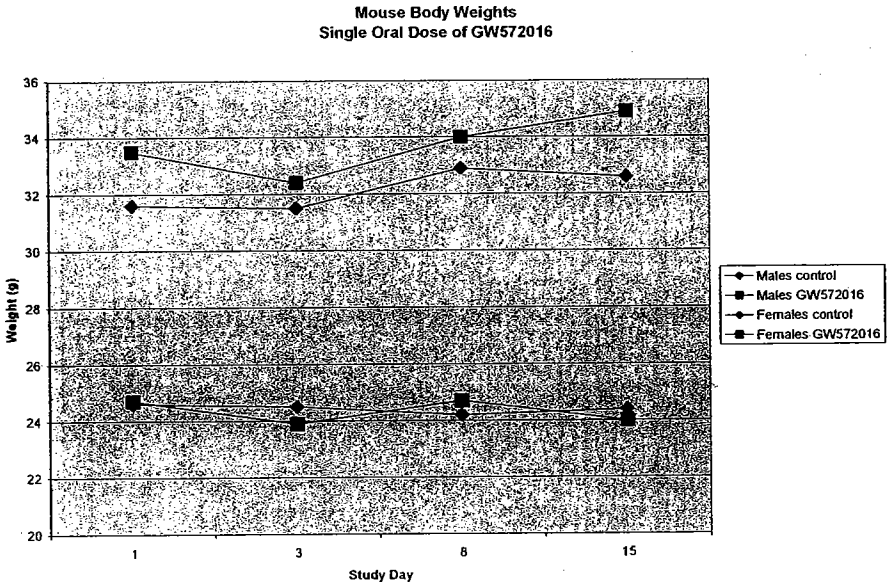

Macroscopically, the only notable finding was a yellow material in the stomach of the treated mice on Day 3, likely corresponding to remaining drug formulation. Microscopically, drug-related findings were seen in the stomach on Day 3 only. These findings include mucus cell hyperplasia in all 6 mice, mucosal atrophy in the glandular stomach of 1/6 and slight focal inflammation in the forestomach in 2/6 mice. These findings were not evident at the Day 15 sacrifice. One female showed clinical signs of slight dehydration.

APPEARS THIS WAY
ON ORIGINAL

RD2000/00479/00: GW572016F: Single-dose intravenous toxicity study in Wistar Han rats

This was a GLP study with two phases. In the first phase 6 rats (3/sex) were administered an IV dose of 25 mg/kg GW572016F, which is the monohydrate form of the ditosylate salt of the active test compound, GW572016X, to determine the maximum nonlethal dose (MNLD). The targeted dose of 25 mg/kg was not achievable due to solubility and dose volume limitations and the rats were actually dosed with 35.5% of the target dose, or 8.9 mg/kg. As no rats died at this dose, it was used for the second phase. In the second phase of the study 6 rats/sex were administered a single IV dose of 25 mg/kg of GW572016. With increased solubility the dose achieved was 84.8% of the target and the rats were administered 21.2 mg/kg. Rats were dosed on Day 1. Three rats/sex of both control and drug groups were euthanized on Day 3, 3/sex were euthanized on Day 15. No lethality was seen in the study. No significant effect was seen on body weights, as noted in the figure below. No clinical signs, microscopic or macroscopic effects of GW572016 treatment were noted.

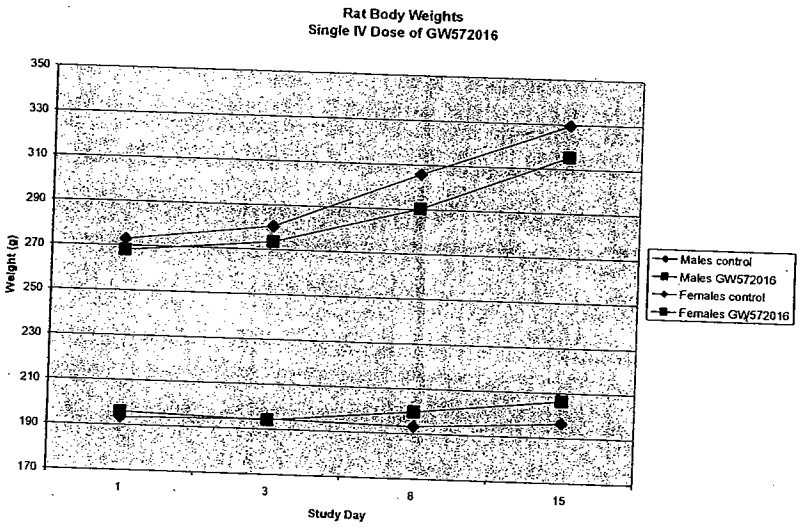

APPEARS THIS WAY
ON ORIGINAL

RD1999/02824/00: GW572016F: Single-dose oral toxicity study in Wistar Han rats
This was a GLP study with two phases. In the first phase 6 rats (3/sex) were administered an oral dose of 2000 mg/kg GW572016F, which is the monohydrate form of the ditosylate salt of the active test compound, GW572016X, to determine the maximum nonlethal dose (MNLD). This dose was chosen based on a repeated dose study in rats where a dose of 1000 mg/kg had no adverse effects following the first day of dosing. As no rats died at this dose in the first phase, it was also used for the second phase. In the second phase of the study 6 rats/sex were administered a single oral dose of 2000 mg/kg of GW572016 on Day 1. Three rats/sex of both control and drug groups were euthanized on Day 3, 3/sex were euthanized on Day 15. No lethality was seen in the study. As noted in the figure below, the rats in the second phase of the study showed a slight reduction in body weights on Day 3 and slightly reduced body weight gain until Day 8 in the female rats.

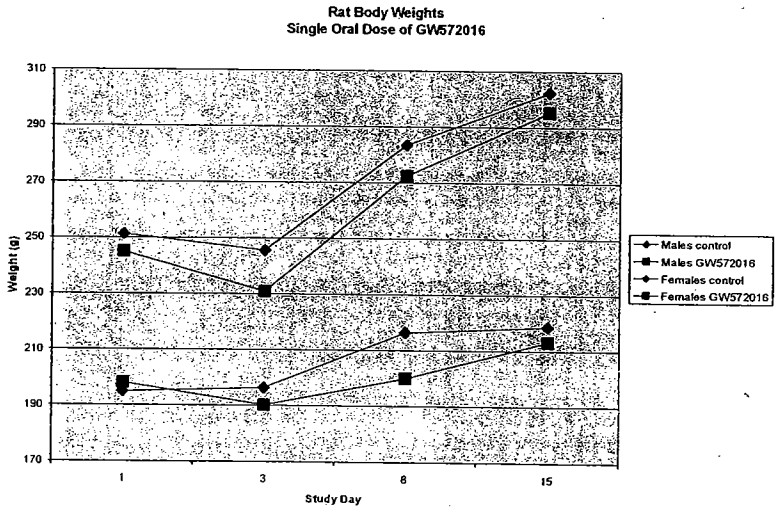

Clinical signs included loose feces and red staining of the snout in 2 drug treated rats in the first phase of the study. Macroscopic findings related to drug treatment are limited to yellow material in the stomach and a watery material in the cecum. The yellow material is likely accumulation of the drug formulation. Microscopic findings are also limited to the GI tract. Day 3 necropsy showed mucosal atrophy in the glandular stomach and duodenum, primarily in the female rats and not evident at Day 15. Diffuse mucosal inflammation was seen on Day 3 in 3/6 drug treated rats and 1/6 of the control rats, not noted at Day 15.

RD2005/01535/00: — Acute oral toxicity in the rat – fixed dose method

A single dose of 300 mg/kg — , an — impurity in the final drug product, was administered to one female rat orally and no toxicity was noted in body weights over a 14-day period, clinical observation, mortality or necropsy. Following that, another female rat was given 2000 mg/kg — with no toxicity so an additional four female rats were administered — at a dose of 2000 mg/kg. No signs of

toxicity were noted at 2000 mg/kg of — indicating that the LD_{50} for — is higher than 2000 mg/kg.

RD2006/01224/00: — Acute oral toxicity in the rat – fixed dose method

A single dose of 500 mg/kg — an — present as an impurity in the final drug product, was administered to one male and one female rat orally and no lethality or clinical signs of toxicity were noted. Following that, another two rats was given 2000 mg/kg — and both rats were euthanized moribund two days after dosing. The main study included 10 rats (5/sex) dosed with 500 mg/kg of — None of the rats died but clinical observations included pallor, hunched posture, lethargy, piloerection, and labored breathing with decreased respiratory rate. Body weights were not affected by drug treatment and no abnormalities were seen upon necropsy. The oral LD_{50} for — in the rat is between 500 and 2000 mg/kg and 500 mg/kg was chosen for the definitive 28-day toxicology study with —

2.6.6.3 Repeat-dose toxicity

Study title: GW572016F: 14-Day oral gavage dose-range-finding toxicity study in CD-1 mice

Key study findings:

- This was a pilot study to examine a dose-range in the mouse
- The HD of 1000 mg/kg was too toxic and mice were euthanized prior to the end of the study
- Some indications of anemia from GW572016 administration

Study no.: RD2001/01439/00

Volume #, and page #:	Module 4.2.3.2.1
Conducting laboratory and location:	GlaxoSmithKline Safety Assessment Five Moore Drive Research Triangle Park, NC 27709
Date of study initiation:	6 November 2001
GLP compliance:	Not GLP
QA reports:	yes ( ) no (X)
Drug, lot #, and % purity:	GW572016F, lot #R5361/44/1 — , purity

Methods

Doses:	100, 300, 1000 mg/kg
Species/strain:	Mouse/CD-1
Number/sex/group or time point (main study):	10/sex/dose
Route, formulation, volume, and infusion rate:	PO, 0.5% hydroxymethylcellulose + 1% Tween 80, 10 mL/kg

Satellite groups used for toxicokinetics or recovery:	6/sex/dose for control 42/sex/dose for GW572016 groups
Age:	6-7 weeks
Weight:	21.6 - 38.2 ♂ 17.4 – 31.3 ♀
Sampling times:	Weeks 4 and 13 at 0, 0.5, 2, 4, 8 and 12 hrs post treatment.

Observation times and results

Mortality: Twice daily

All mice treated with HD were euthanized on Day 8 due to signs of toxicity

Clinical signs: Prior to administration and then 1-2 hrs after administration, with detailed exams given prior to the start of the study and prior to necropsy

Clinical Signs Noted in High Dose GW572016 Mice on Day 7/8 During 14 Day GW572016 Administration in Mice

	Number of ♂ mice	Number of ♀ mice
Pale extremities	10/10	8/10
Decreased activity	2/10	2/10
Loss of skin elasticity	1/10	1/10
Cold to touch	---	1/10

On day 14/15, one MD ♂ mouse also had pale extremities, decreased activity and loss of skin elasticity.

APPEARS THIS WAY
ON ORIGINAL

Body weights: Day -7, 1, 8, 14, 15, 16

Significant body weight loss was seen in the male and female HD mice prior to termination. No other treatment-related body weight changes were seen. The graphs below show the effect of GW572016 on mouse body weights.

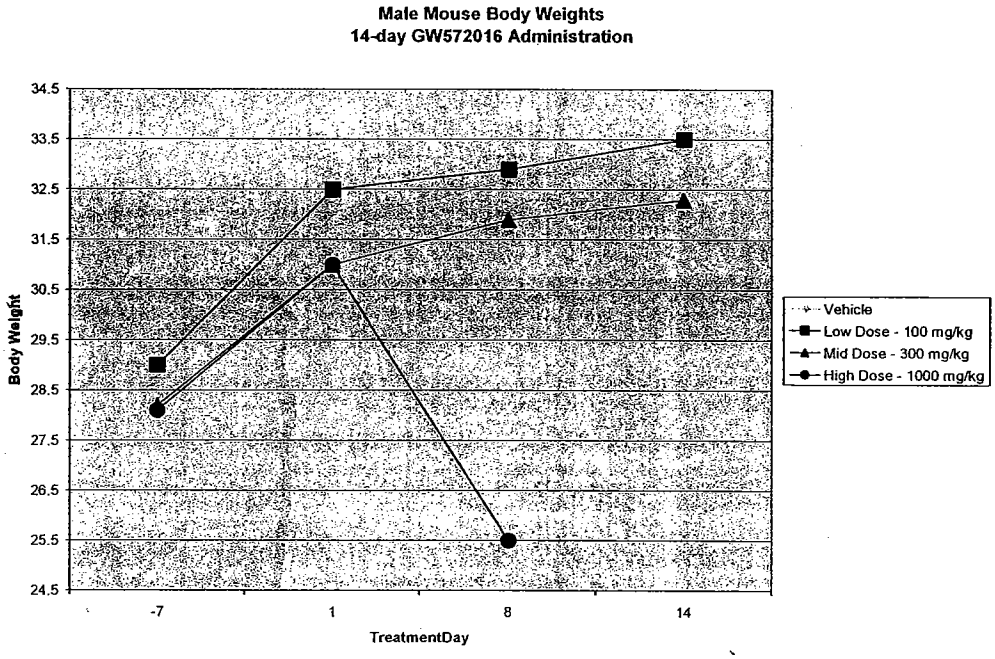

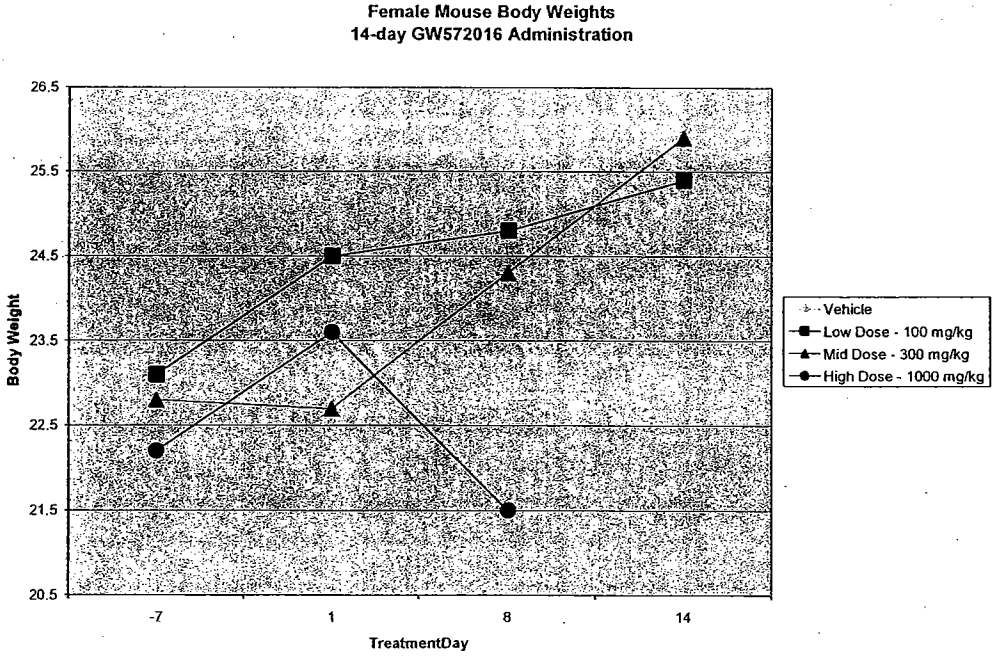

Food consumption: 3 Weekly measurements starting on Day -7

Food consumption data are presented in the figures below. A treatment-related decrease in food consumption is seen in the HD mice during the dosing period from Day 1 – Day 8. These mice were euthanized on Day 8 and the decrease in food consumption and body weights are evidence of the drug's toxicity.

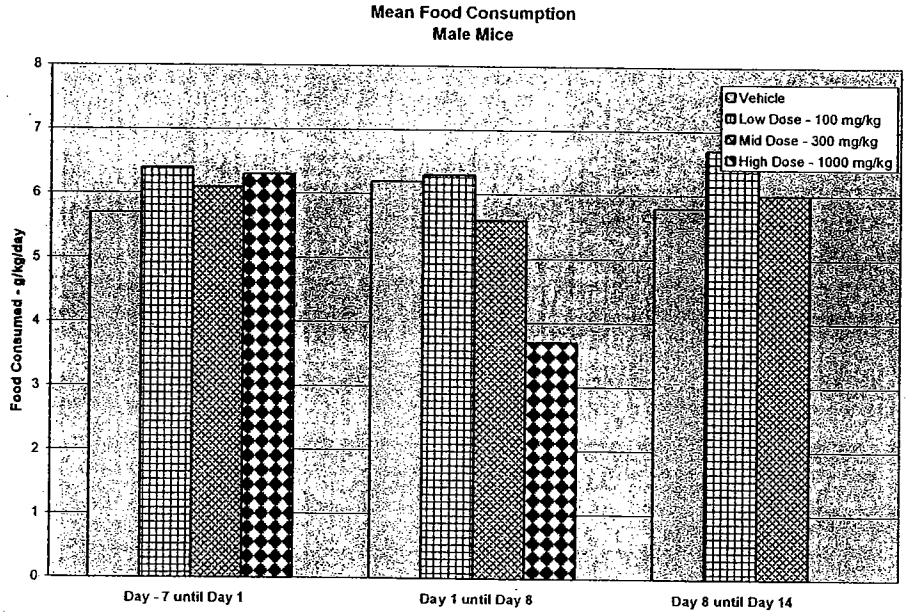

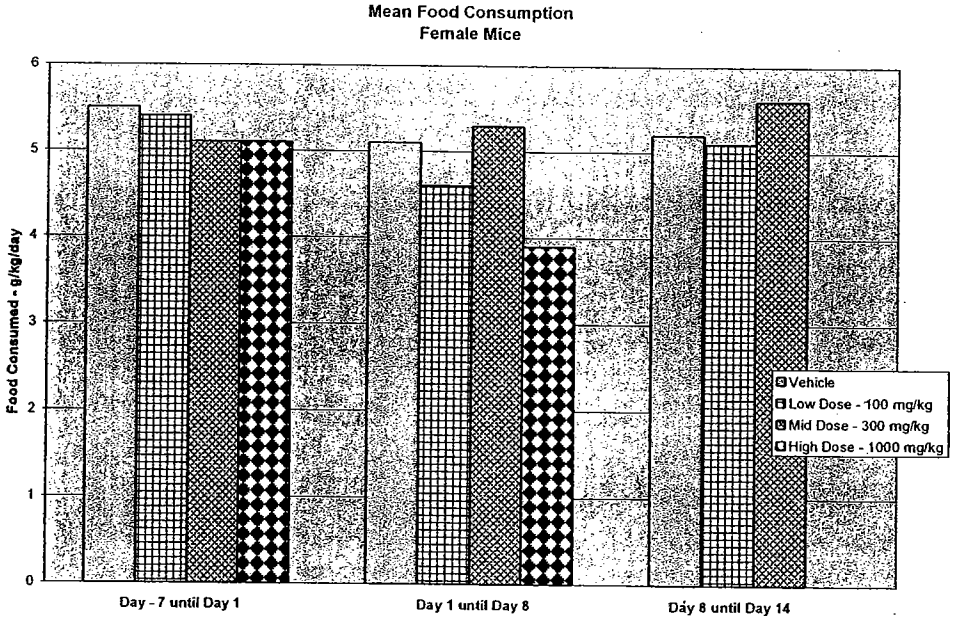

Ophthalmoscopy: Not conducted

EKG: Not conducted

Hematology: At necropsy

The sponsor's table below shows the relevant changes in hematology seen at the completion of 14 days of dosing with GW572016 in male and female mice. One male mouse in the MD group was excluded due to severe anemia. The values for this mouse are presented below the sponsor's table.

Hematology Data Summary (Excluding [redacted], 300 mg/kg/day male)

Sex	Male			Female		
Dose (mg/kg/day)	0	100	300	0	100	300
Number of animals	4	3	4	4	5	3
	Group Mean			Group Mean		
MCV (fL)	54.50	55.03	55.58	54.30	56.50	55.30
RDW (%)	12.05	12.13	12.10	12.00	12.66	12.93
Reticulocytes (%)	2.43	2.80	2.50	2.22	2.72	3.30
Reticuloctyes (x 10^6/µl)	0.2250	0.2367	0.2295[1]	0.1965	0.2302	0.2970
Neutrophils (x 10^6/µl)	0.578	0.713	0.605	0.478	0.626	0.623

[1] N = 4

Individual Mouse Hematology 14 Day GW572016 Administration in Mice Severe Regenerative Anemia	
Hematology Parameter	**Male Mouse [redacted]**
MCV (fL)	73.5
RDW (%)	24.7
Reticulocytes (%)	---
Reticulocytes (x 10^6/µL)	---
Neutrophils (x 10^6/µL)	1.34
Hematocrit (%)	17.9
Hemoglobin (g/dL)	3.7
RBC (x 10^6/µL)	2.44
MCHC (g/dL)	20.7

Clinical chemistry: At necropsy

No treatment-related effects on clinical chemistry parameters

Urinalysis: Not conducted